

Supporting Information

**2-Formylpyridyl Ureas as Highly Selective
Reversible-Covalent Inhibitors of Fibroblast
Growth Factor Receptor 4**

Thomas Knoepfel, Pascal Furet, Robert Mah, Nicole Buschmann, Catherine Leblanc,
Sebastien Ripoche, Diana Graus-Porta, Markus Wartmann, Inga Galuba, Robin A.
Fairhurst*

Novartis Institutes for BioMedical Research, CH-4002 Basel, Switzerland.

Table of contents

Melting point and physicochemical measurements.....	2
Modeling the FGFR4 interactions of selected 2FPU analogues.....	7
FGFR4 biochemical assays.....	12
Kinase selectivity of selected 2FPUs.....	13
Cellular FGFR4 Ba/F3 assay.....	15
FGFR4 kinetic binding assay.....	16
Investigating FGFR4 biochemical assay preincubation times.....	21
Compound synthesis.....	23
X-Ray structure of compound 6b	53
Supporting information abbreviations.....	64
Supporting information references.....	65

Melting point and thermodynamic solubility measurements for the quinoline amide **5** and THNU **6a**.

The melting points of compounds **5** and **6a** were measured by differential scanning calorimetry (DSC) and the thermodynamic solubility (Therm Sol) using the shake-flask method, as described below.

Differential Scanning Calorimetry

Method: Melting point were determined by DSC using a DSC Q2000 (TA Instruments Ltd.) equipped with a refrigerated cooling system (RCS90, TA Instruments). Samples were weighed (about 0.2-0.6 mg) in low mass pans (Tzero Low-Mass Pans, TA Instruments) and clamped with lids (Tzero Lids, TA Instruments) using a sample encapsulating press (Tzero press, TA Instruments). Pans were then manually put into the DSC autosampler together with an empty pan (reference). For each measurement a sample was automatically transferred into the furnace together with the reference pan. The system was first heated using a linear gradient of 50 °C/min from -40 °C to 350 °C. At the end of the measurement a thermogram containing the temperature and heat flow associated with material transitions was automatically registered. The same compound was then repeated using a linear gradient of 10 °C/min starting with new sample material. The melting point (T_m in °C) and Heat of fusion (ΔH in kJ/mol) are extracted from the thermogram, Figures S1 and S2.

Figure S1. DSC thermogram for compound **5**.

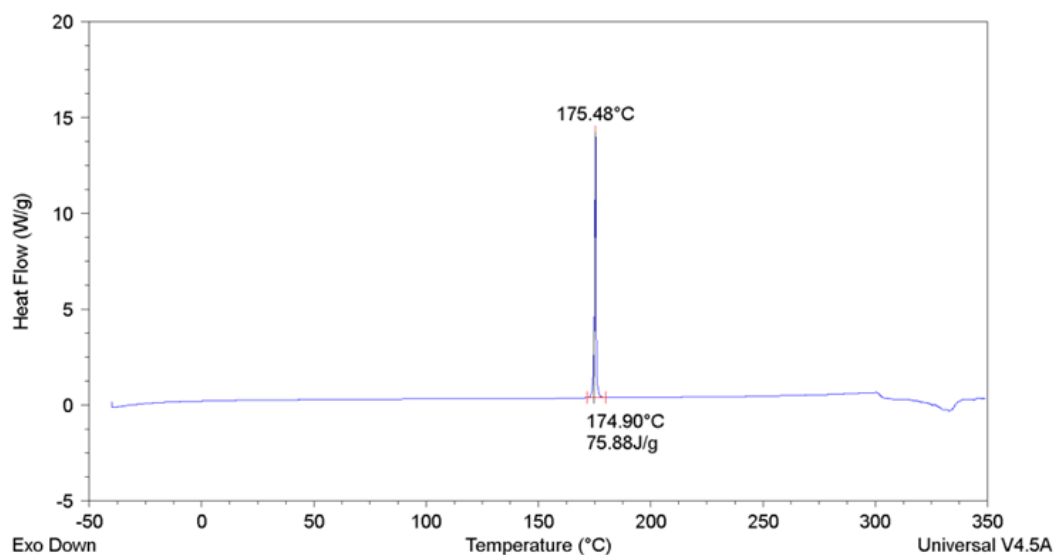
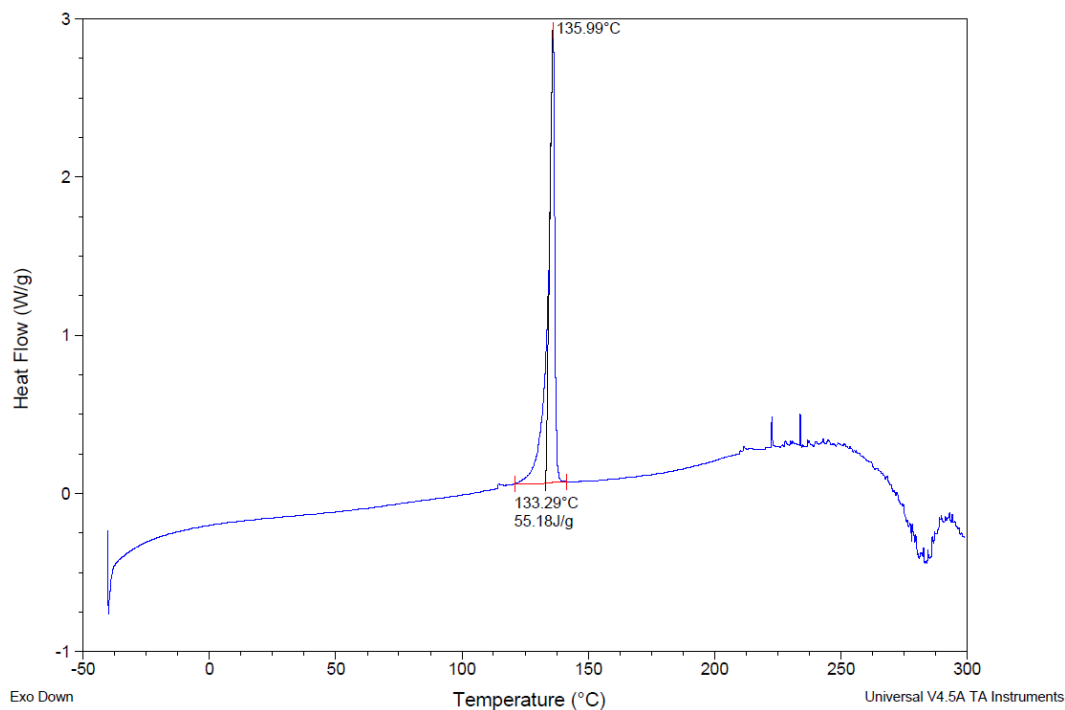


Figure S2. DSC thermogram for compound **6a**.



Shake-flask solubility

The samples were weighted into 2 ml glass vials prior to pH 6.8 phosphate buffer addition to obtain a nominal concentration of 2 mg/ml. The samples were sonicated for 5 minutes and shaken overnight at 1000 rpm (Titrimax 1000, Heidolph) at room temperature. A first phase separation of supernatant and undissolved solid was performed by centrifugation at 3600 rpm during 15 minutes (Eppendorf Centrifuge 5804). The supernatant was then transferred into a conical glass vial for a second centrifugation. An adequate dilution was made of the particle free supernatant and quantified by LC-HRMS using a 6 point calibration curve (Vanquish coupled to an Exactive-Plus, Thermo Scientific).

Table S1. Melting point and thermodynamic solubility data for compounds **5** and **6a**.

Compound	5	6a
Melting point (°C)	175	133
Heat of fusion (kJ/mol)	76	55
Therm Sol pH1.0 (g/l)	3	42
Therm Sol pH6.8 (g/l)	< 1	1.7

Analysis of the solid state interactions

To understand the validity of the hypothesis for increasing solubility by introducing saturation into the quinoline-amide hit **5**, an analysis of the single-crystal X-ray structure of **5**, and the closest THNU analogue **6** for which an X-ray structure was available, were compared. Although not a matched pair, due to differences between the 5-pyridyl substituent, changes in the intermolecular packing observed between **5** and **6b** are consistent with the saturation hypothesis (ref. 11 in the main text).

Figure S3. Intermolecular stacking interactions determined from the X-ray structure of **5**.

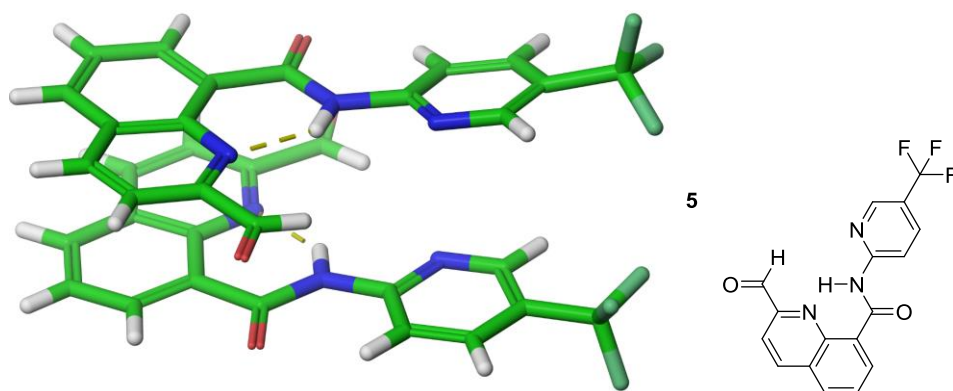
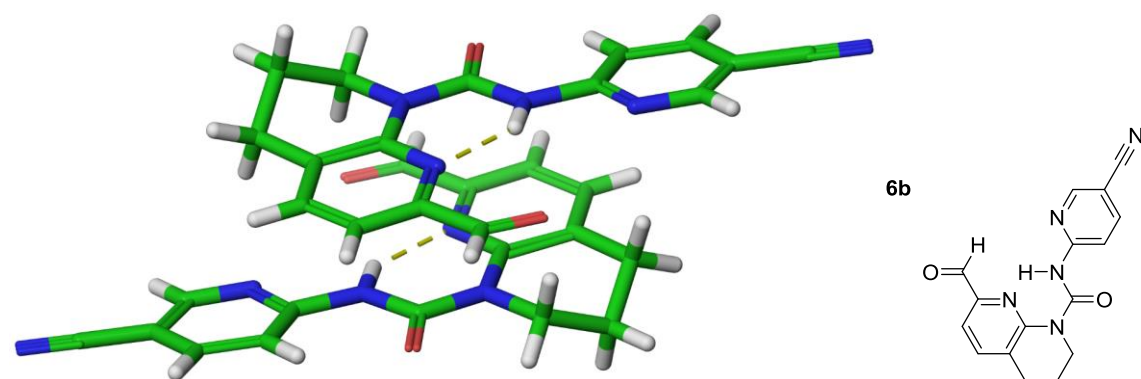


Figure S4. Intermolecular stacking interactions determined from the X-ray structure of **6b**.



In the X-ray crystal structure of compound **5** the molecules are stacked in a head-to-head arrangement, in which both the quinoline and pyridine moieties are involved in π - π -stacking interactions. In the X-ray crystal structure of compound **6b** the molecules are stacked in a head-to-tail arrangement, in which only the urea and 2-formyl pyridine moieties are involved in π - π -stacking interactions. The reduced level of inter-layer π - π -stacking would be consistent with a lower lattice energy, and offer an explanation for the increased solubility observed for **6b**.

Table S2. Physicochemical data for the 2-FPU analogues and reference compounds.

Compound	High-throughput equilibrium solubility pH 6.8 (μM)	log PAMPA (10^{-6} cms^{-1})	clogP	logD _{7.4}	HPLC logD _{7.4}
1	107	- 4.9	3.96	-	-
BLU9931	< 4	- 4.1	6.32	4.2	3.8
5	< 4	- 4.2	2.88	4.9	-
6a	< 4	- 4.0	2.72	3.7	4.1
6b	8	- 3.4	1.29	2.8	2.9
6c	-	-	2.52	-	3.7
6d	48	- 3.9	1.77	-	2.4
6e	11	- 4.3	1.66	1.8	3.1
6f	< 4	- 4.0	2.50	-	-
6g	6	- 3.4	1.55	3.0	3.0
6h	300	- 3.7	1.76	2.1	2.2
6i	-	- 3.4	1.66	-	-
6j	< 4	- 3.7	1.30	2.2	3.0
6k	5	- 3.9	1.11	-	-
7a	69	-	0.35	1.5	-
7b	8	-	0.55	-	-
7c	> 1000	- 4.3	1.06	1.9	-
7d	85	- 4.0	0.45	1.7	1.0
7e	94	- 4.4	1.61	2.3	1.2
7f	< 4	- 4.1	3.57	-	3.0
7g	44	-3.4	1.82	3.0	-
8	> 1000	-	2.46	2.2	-
9	< 4	- 3.7	2.46	-	-
10a	< 4	- 4.1	0.93	-	-
10b	< 4	- 3.8	2.09	3.4	3.2
11a	300	- 3.8	1.85	2.0	-
11b	4	- 3.6	2.11	2.1	-
12a	13	- 4.5	1.77	2.3	2.2
12b	323	- 3.4	1.75	-	-
13	17	- 3.4	0.88	-	-
14	173	- 3.6	1.94	2.4	2.3

High throughput equilibrium solubility was measured using a minaturised shake-flask approach with streamlined HPLC analysis.^{S1}

Permeability and $\log D_{7.4}$ values were measured using a parallel artificial membrane assay (PAMPA).^{S2} For the majority of the 2-FPU analogues high absorbed fractions from the digestive tract were calculated (> 90%) using the PAMPA permeability data. The only exception being **12a**, where the calculated fraction absorbed was 88%.

LogP values were calculated using clogP version 7.4 software: BioByte Corporation.

HPLC $\log D_{7.4}$ values were measured using a HPLC method.^{S3}

Modeling the FGFR4 interactions of selected 2-FPU analogues

At the initiation of this project, no crystal structure of the kinase domain of FGFR4 was available. Therefore, to support the project a model of this domain was generated by homology to the crystal structure of imatinib in complex with FGFR1 (PDB code: 3TT0). The sequences of the human FGFR1 and FGFR4 kinases were obtained from SWISS-PROT,^{S4} entries P11362 and P22455, respectively. The sequences were aligned using T-Coffe.^{S5} On the basis of the resulting alignment, the 3D structure of the FGFR4 kinase was modeled using the 'WHAT IF' program with the default parameters (PIRPSQ module, BLDPIR command).^{S6} Modeling and docking using the homology model was performed with a version of MacroModel enhanced for graphics by A. Dietrich.^{S7} The compounds were manually constructed and docked in the ATP site of the model and the resulting ligand-protein complexes energy-minimized using the AMBER*/H₂O/GBSA force field.

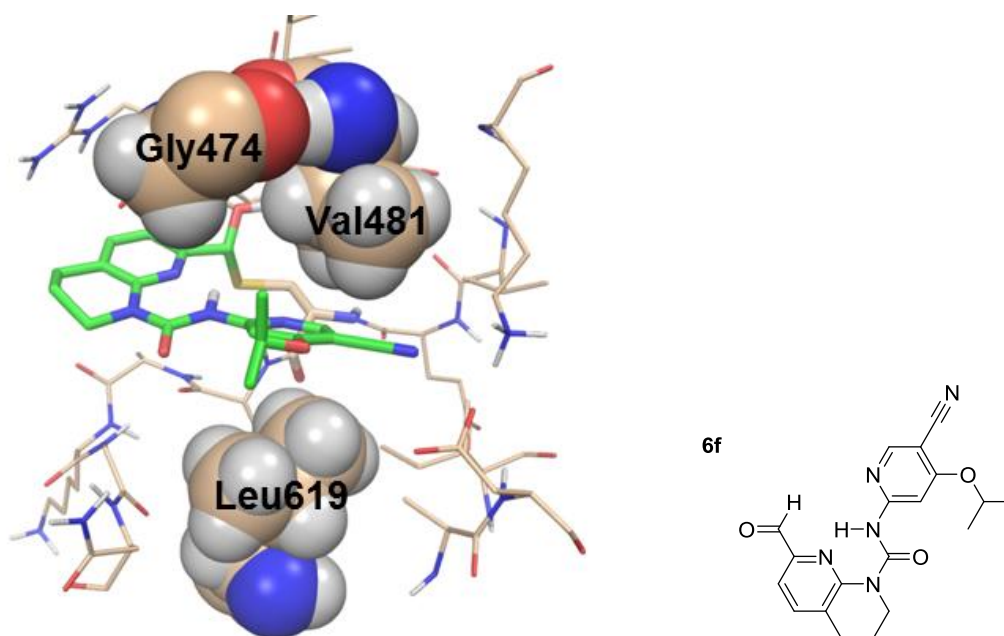


Figure S5. Model of **6f** bound within the ATP binding site of FGFR4. The hydrophobic interactions between the isopropoxy moiety of **6f** with Leu619 and the hydrophobic crevice formed between Gly474 and Val481 are highlighted.

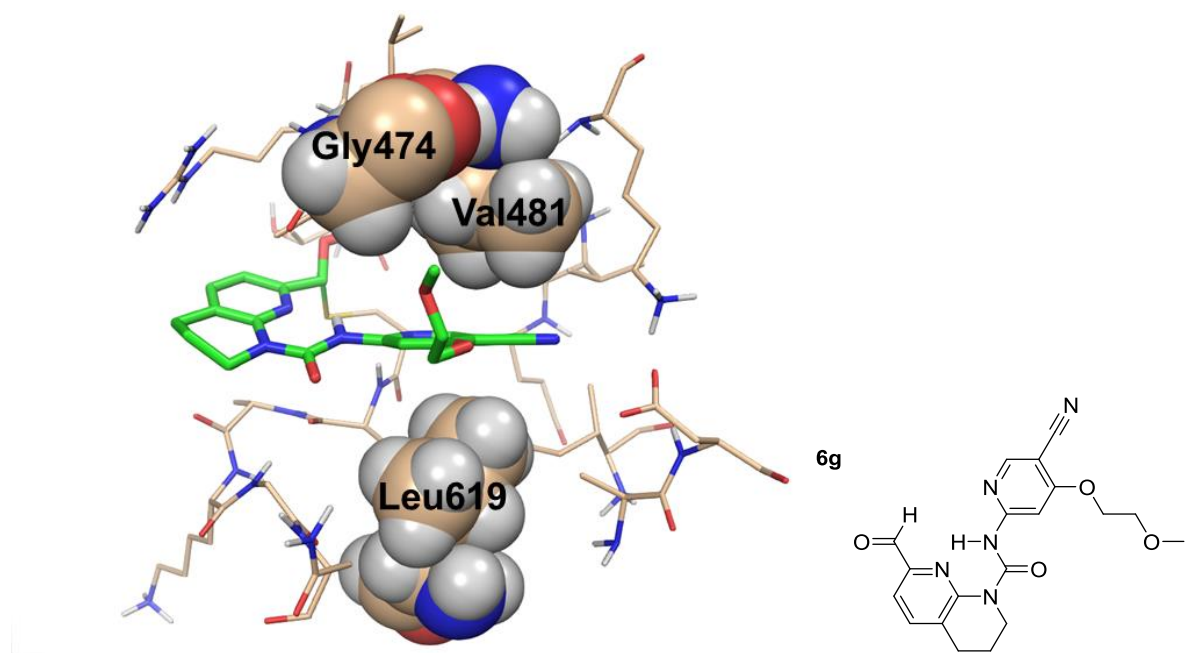


Figure S6. Model of **6g** bound within the ATP binding site of FGFR4. The hydrophobic interactions between the methoxyethoxy moiety of **6g** with Leu619 and the hydrophobic crevice formed between Gly474 and Val481 are highlighted.

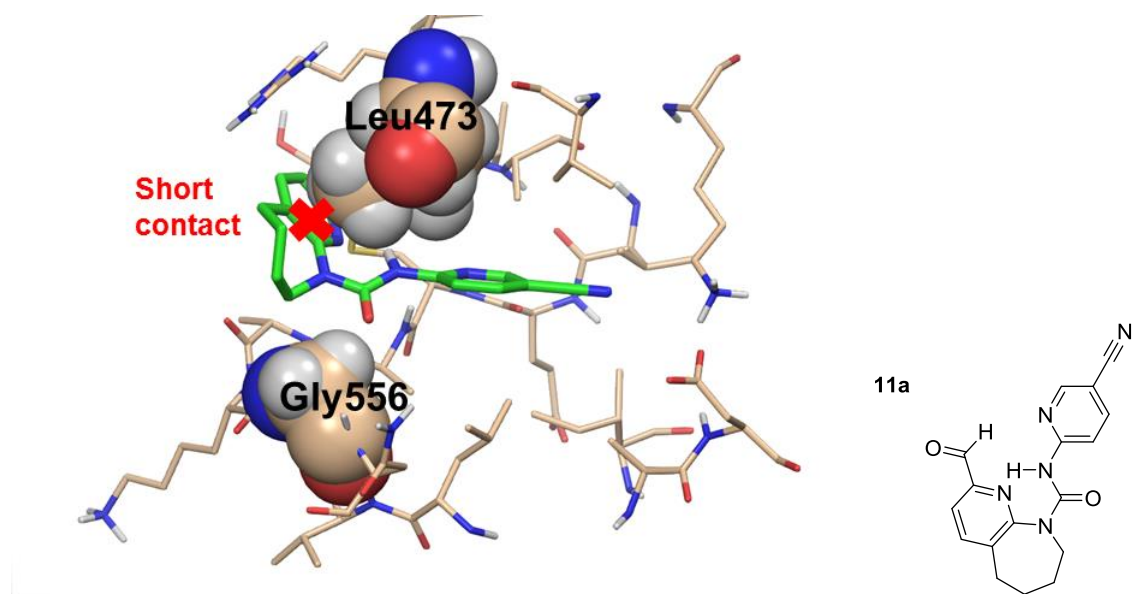


Figure S7. Model of **11a** bound within the ATP binding site of FGFR4. The unfavorable interaction resulting from the larger 7-membered ring binding within the hydrophobic slot, formed by residues Leu473 and Gly556, is highlighted.

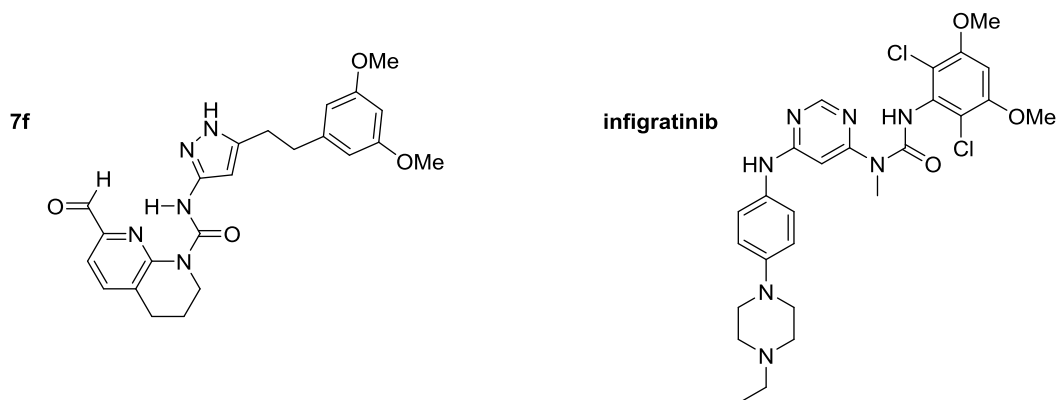
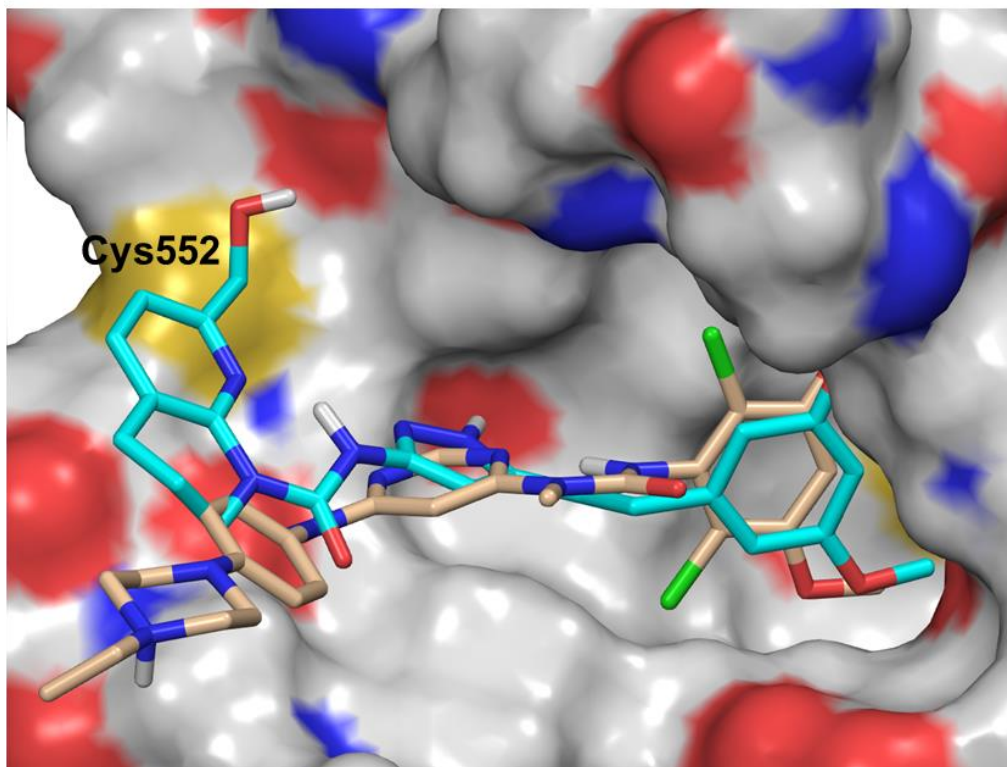


Figure S8. Model of **7f** (turquoise structure) bound within the ATP binding site of FGFR4 and overlaid with the X-ray structure of infigratinib (beige structure, PDB ID: 3TT0). The overlay highlights the back pocket interactions made by the 3,5-dimethoxyphenyl moieties of both compounds, which is common to a number of reported FGFR inhibitors.

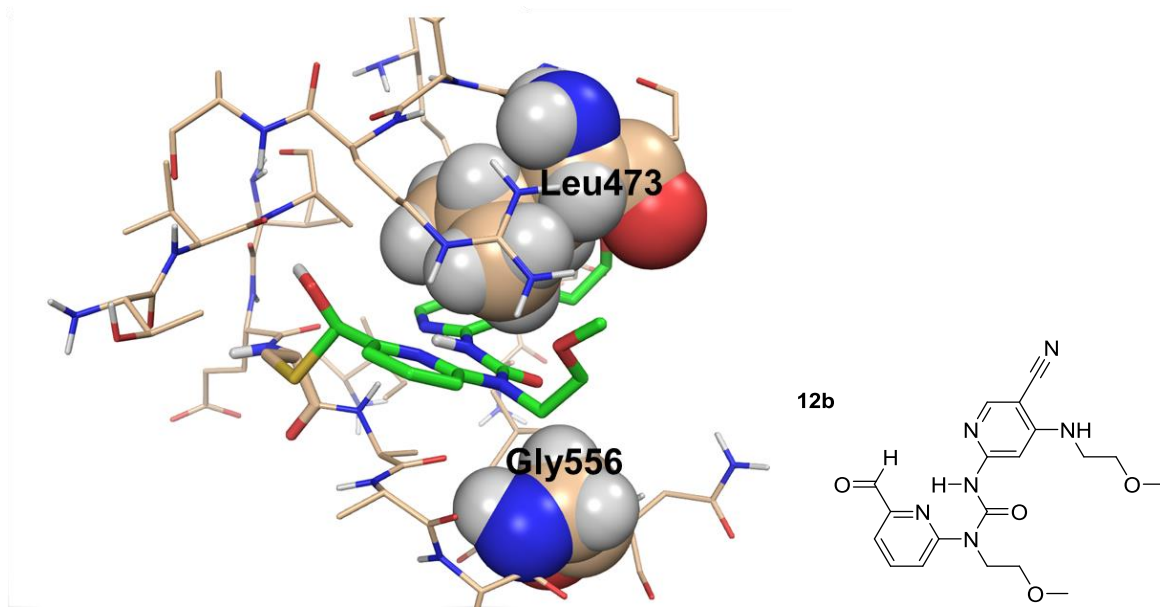


Figure S9. Model of **12b** bound within the ATP binding site of FGFR4. The orientation of the urea *N*-methoxyethyl moiety into solvent is indicated, and highlights the opportunity for incorporating a range of substituents at this position.

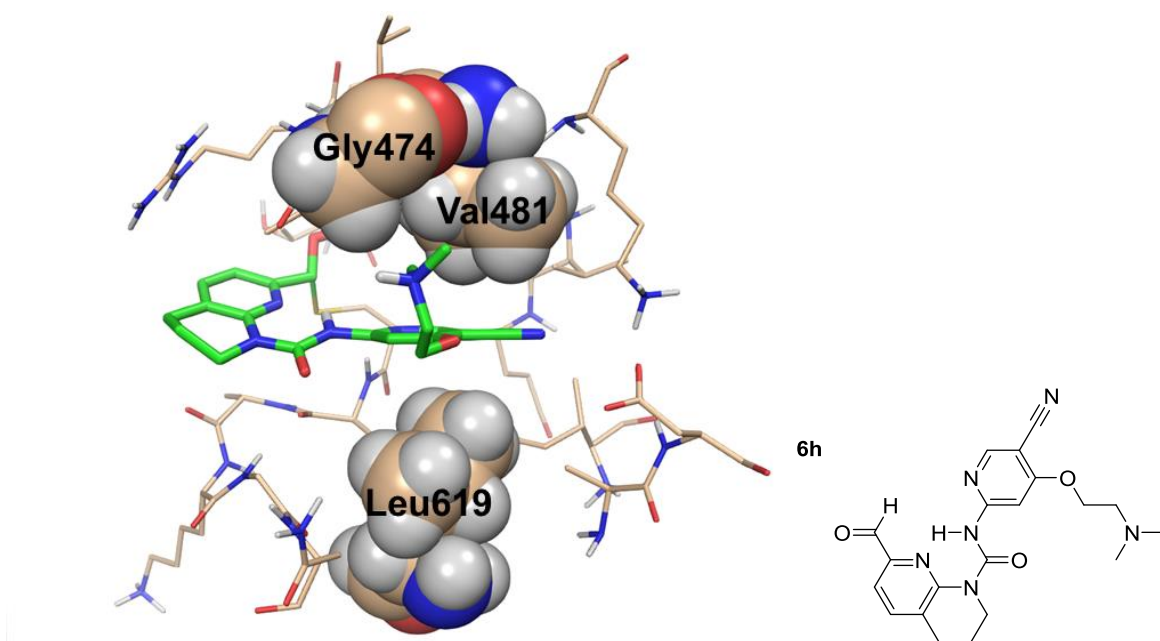


Figure S10. Model of **6h** bound within the ATP binding site of FGFR4. The hydrophobic interactions between the dimethylaminoethoxy moiety of **6h** with Leu619 and the hydrophobic crevice formed between Gly474 and Val481 are highlighted.

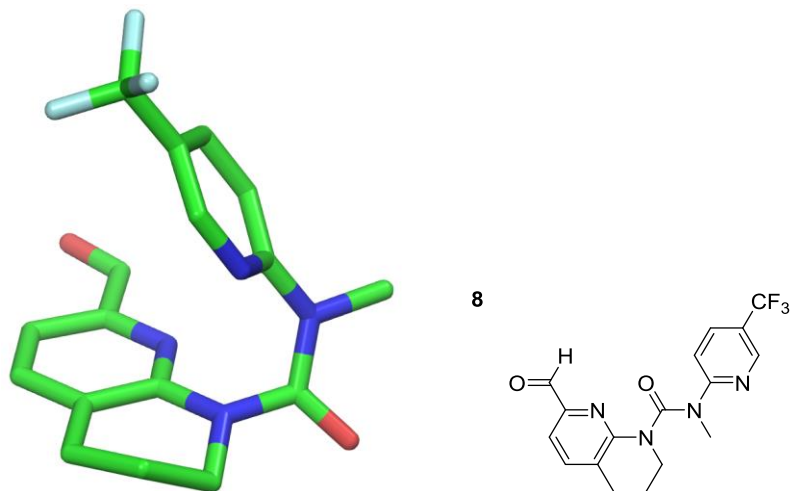


Figure S11. Representation of the lowest energy conformation for compound **8** calculated using the MCM/OPLS 2005/H₂O method in the MacroModel module of Maestro (Schrodinger Inc.). The conformations with a *trans*-amide bond (required for the active FGFR4 binding conformation) are of higher energy (more than 5 kcal/mol above the lowest energy conformation represented above).

Kinase assays

FGFR 'biochemical assay 'standard screening conditions' (Table 1 in main text and Table S3)

All assays were performed in 384-well small volume microtiter plates (Greiner bio-one, Cat. No. 784076). Each assay plate contained 8-point serial dilutions for 40 test compounds, as well as four 8-point serial dilutions of staurosporine as a reference compound, plus 16 high- and 16 low controls.

Liquid handling and incubation steps were done on an Innovadyne Nanodrop Express equipped with a robotic arm (Thermo CatX, Caliper Twister II) and an incubator (Liconic STX40, Thermo Cytomat 2C450). The assay plates were prepared by addition of 50 nl per well of compound solution in 90% DMSO. The kinase reactions were started by stepwise addition of 4.5 μ L per well of enzyme solution (50 mM HEPES pH 7.5, 1 mM DTT, 0.02% Tween20, 0.02% BSA, 10 mM beta-glycerolphosphate, 10 μ M sodium orthovanadate with enzyme specific enzyme / $MgCl_2$ / $MnCl_2$ concentrations, Table S1) and 4.5 μ L per well of peptide/ATP-solution (4 μ M peptide, FGFR1-3 assays used the 5-Fluo-Ahx-EEPLYWSFPAKKK-CONH₂ peptide substrate, and the FGFR4 assays used the 5-Fluo-Ahx-KKKKEEIYFFFG-NH₂ peptide substrate, 50 mM HEPES pH 7.5, 1 mM DTT, 0.02% Tween20, 0.02% BSA, 10 mM beta-glycerolphosphate, 10 μ M sodium orthovanadate with enzyme specific ATP / $MgCl_2$ / $MnCl_2$ concentrations, Table S3). Kinase reactions were incubated at 30 °C for 60 minutes and subsequently terminated by addition of 15 μ l per well of stop solution (100 mM HEPES pH 7.5, 5% DMSO, 0.1% Caliper coating reagent, 10 mM EDTA, and 0.015% Brij35). Plates with terminated kinase reactions were transferred to the Caliper LC3000 system for reading. Phosphorylated and unphosphorylated peptides were separated using the Caliper microfluidic mobility shift technology. Briefly, samples from terminated kinase reactions were applied to the chip. Analytes are transported through the chip by constant buffer flow and the migration of the substrate peptide is monitored by the fluorescence signal of its label. Phosphorylated peptide (product) and unphosphorylated peptide (substrate) are separated in an electric field by their charge/mass ratio. Kinase activities were calculated from the amounts of formed phospho-peptide. IC₅₀ values were determined from percent inhibition values at different compound concentrations by non-linear regression analysis.

Table S3. Details of the biochemical assay conditions.

Kinase domain (sequence)	Enzyme conc (nM)	ATP K _m (μ M)	MgCl ₂ / MnCl ₂ conc (μ M)
FGFR1(407-822)	2	319	12 / 0
FGFR2 (406-821)	3	146	12 / 0
FGFR3(411-806)	0.25	353	12 / 0
FGFR4 (388-802)	3	561	16 / 0
FGFR4 (442-753) nonphos	3	220	18 / 2
FGFR4 (442-C552A-753) nonphos	5	789	16 / 3

Selectivity of the 2FPU analogues 6-14

To assess selectivity biochemical assays were performed with the indicated purified kinases, or recombinant kinase-domains, in the absence and with increasing concentrations of the test compounds by measuring the incorporation of ^{33}P , from $[\gamma\text{-}^{33}\text{P}]\text{ATP}$, into appropriate substrates. All values are from duplicate measurements, and average values are shown from 1 to 3 separate experiments, Table S4.

The assays were performed using Caliper technology and are typically run at ATP K_m for the assay specific enzyme concentration.

The activity with the C552A variant of FGFR4 was assessed using the assay described in reference 4 from the main text.

Table S4. Biochemical kinase inhibitory activities for selected 2-FPU analogues, **5** and the non-covalent reference compound **1**.

Kinase	Compound IC ₅₀ values (μM)									
	1	5	6a	6b	6g	7a	7b	9	10b	12a
FGFR1	0.28	> 10	> 10	> 10	> 10	> 10	> 10	> 10	> 10	> 10
FGFR2	0.36	> 10	> 10	> 10	> 10	> 10	> 10	> 10	> 10	> 10
FGFR3	3.5	> 10	> 10	> 10	> 10	> 10	> 10	> 10	> 10	> 10
C552A FGFR4	0.008	> 10	> 10	> 10	> 10	> 10	-	-	-	-
ABL1	> 10	> 10	> 10	> 10	> 10	> 10	> 10	> 10	> 10	> 10
ACVR1	> 10	> 10		> 10	> 10	> 10	> 10	> 10	> 10	> 10
AKT1	> 10	4.1	9.4	> 10	> 10	> 10	5.1	> 10	> 10	> 10
AURKA	1.9	> 10	> 10	9.1	> 10	> 10	> 10	7.3	> 10	> 10
BTK	> 10	> 10	> 10	> 10	> 10	> 10	> 10	> 10	> 10	> 10
CAMK2D	0.019	> 10	> 10	> 10	> 10	> 10	> 10	> 10	> 10	> 10
CDK1B	> 10	> 10	> 10	> 10	> 10	> 10	> 10	> 10	> 10	> 10
CDK2A	> 10	> 10	> 10	> 10	> 10	> 10	> 10	> 10	> 10	> 10
CDK4D1	5.9	> 10	> 10	> 10	> 10	> 10	> 10	> 10	> 10	> 10
CSK	> 10	> 10	> 10	> 10	> 10	> 10	> 10	> 10	> 10	> 10
CSNK1G3	3.9	> 10	> 10	> 10	> 10	> 10	> 10	> 10	> 10	-
EGFR	0.051	> 10	> 10	> 10	> 10	> 10	> 10	> 10	> 10	> 10
EphB4	> 10	> 10	> 10	> 10	> 10	> 10	> 10	> 10	> 10	> 10
ERBB2	0.25	-	-	-	-	-	-	-	-	-
ERBB4	-	> 10	> 10	> 10	> 10	> 10	> 10	> 10	> 10	> 10
FLT3- D835Y	0.37	> 10	7.9	> 10	> 10	> 10	> 10	> 10	> 10	> 10
GSK3B	> 10	> 10	> 10	> 10	> 10	> 10	> 10	> 10	> 10	> 10
INSR	0.46	> 10	> 10	> 10	> 10	> 10	> 10	> 10	> 10	> 10
IRAK1	> 10	> 10	-	-	> 10	> 10	-	> 10	> 10	> 10
IRAK4	> 10	> 10	-	> 10	> 10	> 10	> 10	> 10	> 10	> 10
JAK1	> 10	> 10	> 10	> 10	> 10	> 10	> 10	> 10	-	> 10
JAK2	> 10	> 10	> 10	> 10	> 10	> 10	> 10	> 10	> 10	> 10
JAK3	-	-	> 10	> 10	-	-	-	-	-	-
KDR	0.54	> 10	> 10	> 10	> 10	> 10	> 10	> 10	-	> 10
KIT	> 10	> 10	> 10	> 10	> 10	> 10	> 10	> 10	-	> 10
LCK	> 10	> 10	> 10	> 10	> 10	> 10	> 10	> 10	> 10	> 10

Compound	1	5	6a	6b	6g	7a	7b	9	10b	12a
LYN	> 10	> 10	> 10	> 10	> 10	> 10	> 10	> 10	> 10	> 10
MAP3K8	> 10	> 10	> 10	> 10	> 10	> 10	> 10	> 10	-	> 10
MAPK14	-	-	-	> 10	> 10	> 10	> 10	> 10	> 10	> 10
MAPK1	8.3	> 10	> 10	> 10	> 10	> 10	> 10	> 10	> 10	> 10
MAPK10	-	-	-	> 10	> 10	> 10	> 10	> 10	> 10	> 10
MAPKAPK2	> 10	2.3	> 10	4.4	0.16	> 10	6.3	3.3	-	1.7
MAPKAPK5	1.4	> 10	> 10	> 10	> 10	> 10	> 10	> 10	> 10	> 10
MERTK	-	> 10	-	-	> 10	> 10	-	-	-	-
MET	> 10	> 10	> 10	> 10	> 10	> 10	> 10	> 10	> 10	> 10
MKMK1	> 10	> 10	> 10	> 10	> 10	> 10	> 10	> 10	> 10	> 10
MKMK2	1.5	> 10	> 10	> 10	> 10	> 10	> 10	> 10	-	> 10
PAK2	> 10	> 10	> 10	> 10	> 10	> 10	> 10	> 10	> 10	> 10
PDGFR α	-	> 10	> 10	-	> 10	-	> 10	> 10	-	-
PDGFR α -V561D	0.90	5.9	6.7	> 10	> 10	> 10	> 10	> 10	-	> 10
PDPK1	> 10	> 10	> 10	> 10	> 10	> 10	> 10	> 10	> 10	> 10
PIM2	> 10	> 10	> 10	> 10	> 10	> 10	> 10	> 10	> 10	> 10
PKN1	> 10	> 10	> 10	> 10	> 10	> 10	> 10	> 10	> 10	> 10
PKN2	> 10	> 10	> 10	> 10	> 10	> 10	> 10	> 10	> 10	> 10
PLK1	0.15	> 10	> 10	> 10	> 10	> 10	> 10	> 10	-	> 10
PRKACA	> 10	> 10	> 10	> 10	> 10	> 10	> 10	> 10	> 10	> 10
PRKCA	> 10	> 10	> 10	> 10	> 10	> 10	> 10	> 10	> 10	> 10
PRKCQ	> 10	> 10	> 10	> 10	> 10	> 10	> 10	> 10	> 10	> 10
RET	8.8	> 10	> 10	> 10	> 10	> 10	> 10	> 10	> 10	> 10
ROCK2	1.0	> 10	> 10	> 10	> 10	> 10	> 10	> 10	-	> 10
RPS6KB1	> 10	> 10	> 10	> 10	> 10	> 10	> 10	> 10	> 10	> 10
SRC	> 10	> 10	> 10	> 10	> 10	> 10	> 10	> 10	> 10	> 10
SYK	> 10	> 10	> 10	> 10	> 10	> 10	> 10	> 10	> 10	> 10
TYK2	-	-	> 10	-	-	-	-	> 10	-	-
WNK1	> 10	> 10	> 10	> 10	> 10	> 10	-	> 10	-	> 10
ZAP70	> 10	> 10	> 10	> 10	> 10	> 10	> 10	> 10	> 10	> 10

- = not determined.

From the above list, MAPKAPK2 is the only other kinases which contain a Cys residue at the gate-keeper plus two position.

FGFR4 cellular Ba/F3-TEL assay

As a read out for cellular FGFR4 kinase activity, an assay that measures the extent of FGFR4 tyrosine phosphorylation was developed. The assay employs a BaF3-Tel-FGFR4 cell line which was generated by stably transduced BaF3 cells with a retrovirus encoding a fusion protein consisting of the amino terminal portion of TEL (aa1-337) fused to the cytoplasmic domain of FGFR4, including the juxta membrane domain.^{S8} The presence of the TEL domain results in constitutive activation of the fused FGFR4 kinase by oligomerization, and thus autophosphorylation of the tyrosine sites.^{S9} An MSD (MesoScale Discovery)-based capture ELISA was developed and used as follows: 250'000 BaF3-Tel-FGFR4 cells per well were seeded in 96-well tissue culture plates (Corning Cat# 3359) in 40 µl of growth medium (RPMI-1640 (Amimed Cat#1-41F01-I) supplemented with 10% fetal calf serum, 10 mM HEPES, 1 mM Sodium Pyruvate, 2 mM Stable Glutamine and 1x Penicillin-Streptomycin). Using a liquid handling device (Velocity 11 Bravo, Agilent), serial 3-fold dilutions of compounds were prepared in DMSO, prediluted in growth medium to 5-fold the desired final concentration, followed by transfer of 10 µl/well to the cell plates. After incubation for 1 hour at 37 °C/5%CO₂, 50 µl of lysis buffer (150 mM NaCl, 20 mM Tris (pH 7.5), 1 mM EDTA, 1 mM EGTA, 1% Triton X-100, 10 mM NaF, complemented with protease inhibitors (Complete Mini, Roche Cat# 11836153001) and phosphatase inhibitors (Phosphatase Inhib I, SIGMA Cat# P2850; 30 Phosphatase Inhib II, SIGMA Cat# P5726 according to supplier instructions) was added and incubated for 30 minutes on ice with shaking at 300 rpm. Sample plates were then frozen and stored at -70 °C. Following thawing on ice, the sample plates were centrifuged for 15 minutes at 1200 rpm at 6 °C.

For the ELISA assay, Multi array 96 well plates (MSD, Cat# L15XB-3) were coated for 1 hour at room temperature with 25 ul/well of mouse anti-H-TEL antibody (Santa Cruz, Cat# sc-166835) diluted 1:400 in PBS/O. Following addition of 150 µL of 3% MSD-blocker A (Cat# R93BA-1) in TBS- 260T (50 mM Tris, 150 mM NaCl, 0.02%Tween-20), plates were incubated for 1 hour at room temperature with shaking. Plates were then washed 3 times with 200 µl/well of TBS-T. 50 µl of the cell lysate was then transferred to the coated plate and incubated for 15 hours at 4 °C, followed by 3 washes with 200 ul TBS-T/well and addition of 25 ul/well of MSD SULFOTAGGED PY20 antibody (MSD Cat# R32AP-5), diluted 1:250 in TBS-T + 1% MSD Blocker A. Following Incubation for 1 h at room temperature with shaking, wells were washed 3 times with 200 µl TBS-T/well. Following addition of 150 µl MSD Read Buffer (MSD, Cat# R92TC-2) stock solution diluted 1:4 with nano water, electrochemiluminescent signal generation was immediately quantified on a SectorImager 6000 (MSD). IC₅₀ calculation: For data analysis, the assay background was determined in wells containing medium and lysis buffer, but no cells, and the corresponding value subtracted from all data points. The effect of a particular test compound concentration on FGFR4 phosphorylation is expressed as percentage of the background-corrected electro-chemiluminescence reading obtained for cells treated with vehicle only (DMSO, 0.2% f.c.), which is set as 100. Compound concentrations leading to half-maximal signal inhibition (IC₅₀) were determined by standard four parametric curve fitting (XLfit 5.4, IDBS).

Binding kinetic measurements

Kinetic binding assays were conducted with Proteros GmbH using the Proteros Reporter Displacement Assay.^{S10}

In summary: The Proteros reporter displacement assay is based on reporter probes that are designed to bind to the site of interest of the target protein. The proximity between reporter and protein results in the emission of an optical signal. Compounds that bind to the same site as the reporter probe displace the probe, causing signal diminution. The rate of reporter displacement is measured over time after the addition of the compounds at various concentrations, Figure S12.

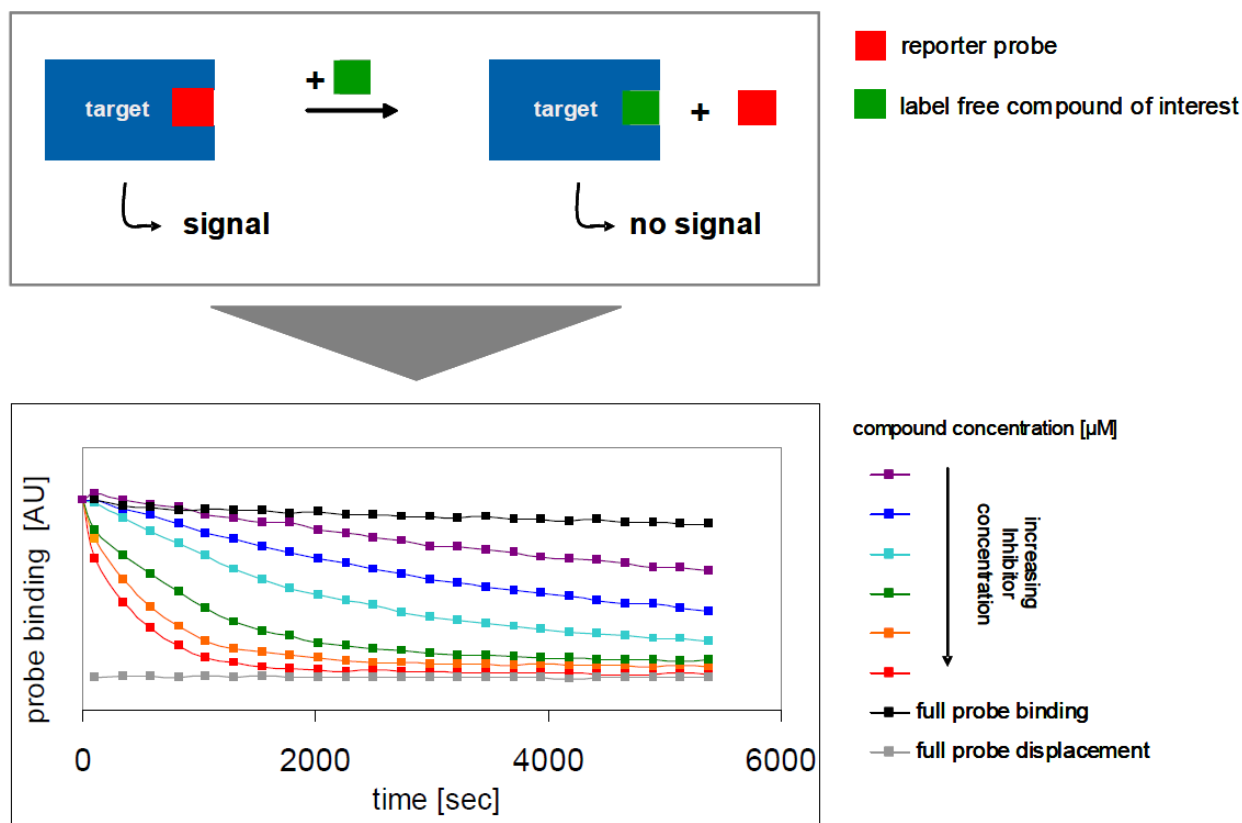
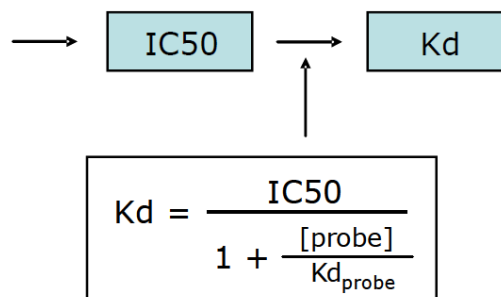
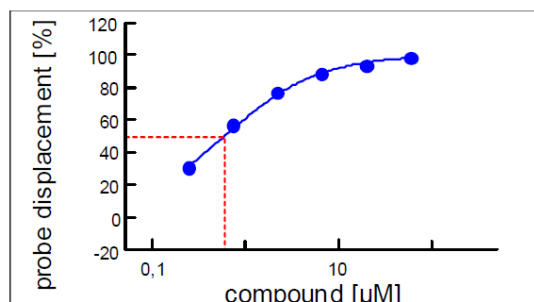


Figure S12. Assay principle of the Proteros Reporter Displacement Assay.

In order to ensure that the rate of probe displacement reflects compound binding and not probe dissociation, probes are designed to have fast dissociation rates. Thus, compound binding and not probe dissociation is the rate limiting step of probe displacement. For K_d determination, percent probe displacement values are calculated for the last time point, at which the system has reached equilibrium. For each compound concentration, percent probe displacement values are calculated and plotted against the compound concentration. IC_{50} -like values (corresponding to 50% probe displacement) are calculated using standard fitting algorithms. The reporter probe is used at a concentration reflecting its own K_d (probe) value. Thus, according to the Cheng Prusoff equation, the K_d value can be calculated with $K_d = \frac{1}{2} IC_{50}$, Figure S13.



Cheng Prusoff Equation

Figure S13. K_d determination.

For determination of binding kinetics (k_{on} , k_{off} , residence time), reporter displacement is plotted against time and fitted to a mono-exponential decay equation (probe binding = $B + A \times \exp(-k_{obs} \times t)$) for each compound concentration. The resulting exponential coefficients equal the apparent association rate k_{obs} . In a secondary plot, the k_{obs} values are plotted against the corresponding compound concentrations. Based on the equation $k_{obs} = k_{off} + k_{on} \times [\text{compound}]$, k_{on} values are extracted from the slope after linear fitting, Figure S14. The k_{off} values are calculated by $K_d(\text{compound}) \times k_{on}$. Residence time of the compound on the protein is calculated by $1/k_{off}$. For the secondary plot, only data are used from compound concentrations at which the k_{obs} values can be clearly determined. Data were omitted from the secondary plot analysis if (1) probe displacement was too fast to calculate accurate k_{obs} values, (2) compound concentration was too low to displace the probe significantly or (3) compound binding was faster than probe dissociation.

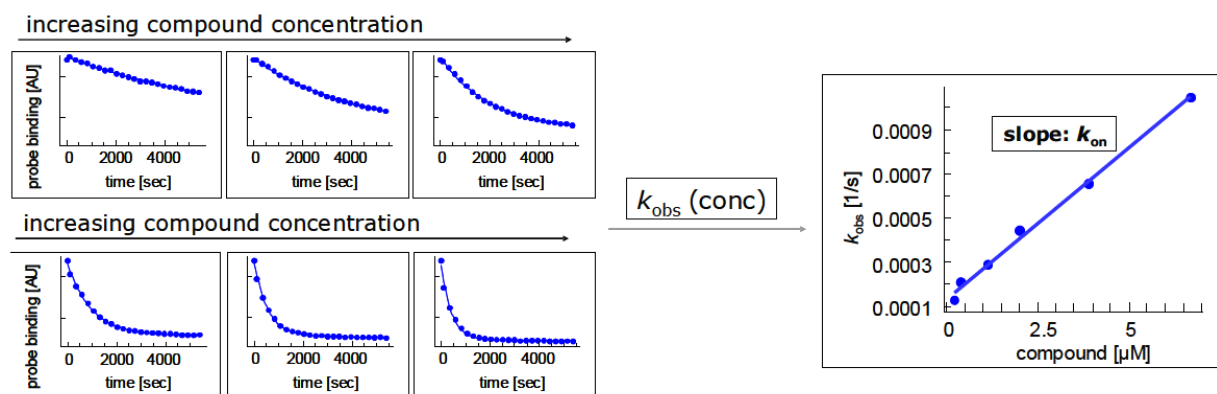


Figure S14. Determination of binding kinetics.

Overview of the assay conditions:

Target enzyme: FGFR4 (391—802), ProQinase 0127-0000-3

Reaction volume: 15 μ l

Reaction temperature: RT

Assay plates: 384 well U bottom, PP, black, low volume (Corning, 3676)

Controls:

Full probe displacement: highest compound concentration

Full probe binding: lowest compound concentration

Reaction buffer:

20 mM Mops, pH 7.0

1 mM DTT

0.01% Tween20

Final assay concentrations:

Target enzyme: 20.0 nM FGFR4

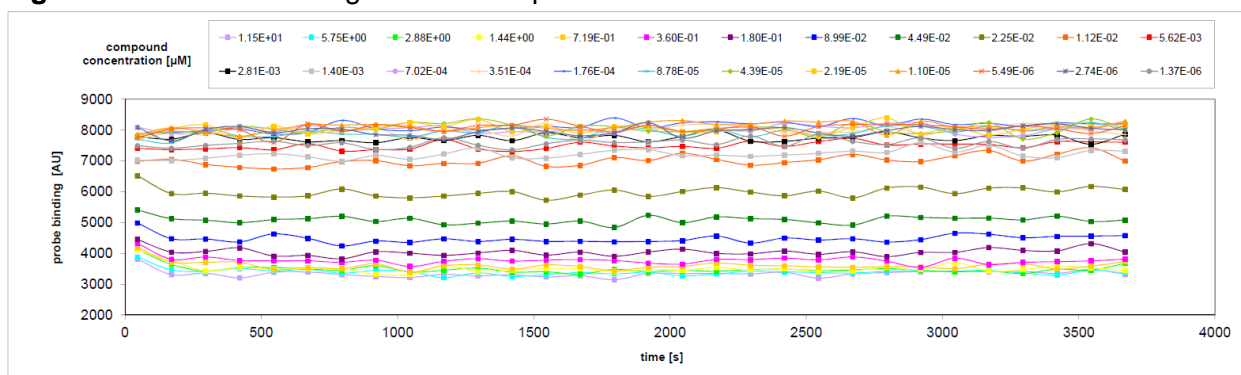
Reporter probe (adjusted to K_d): 489 nM PRO-128 (FGFR4)

Pipetting sequence:

- 1) Add 10 μ l 15/10 fold concentrated target enzyme in reaction buffer
- 2) Add 5 μ l 15/5 fold concentrated reporter probe in reaction buffer
- 3) Incubate for 30 min
- 4) Add inhibitor in 100% DMSO
- 5) Measure time dependence of reporter displacement

Results: All compounds with slow binding mode followed classical mono-exponential binding kinetics.

Figure S15. Kinetic binding data for compound 1.



IC50:

time point [s]	IC50 [μM]	Kd [μM]
3670	3.97E-02	1.98E-02

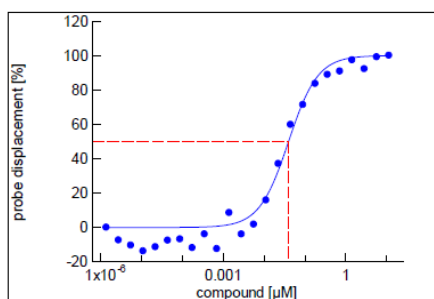
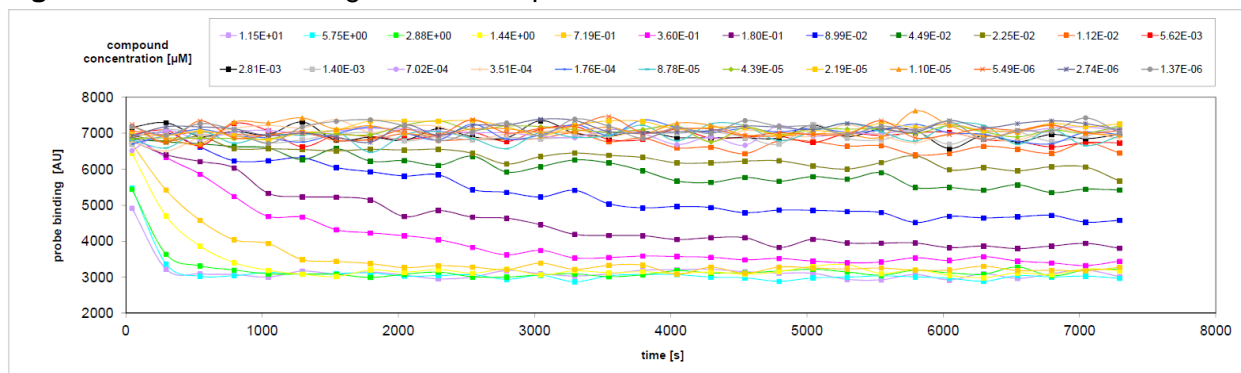
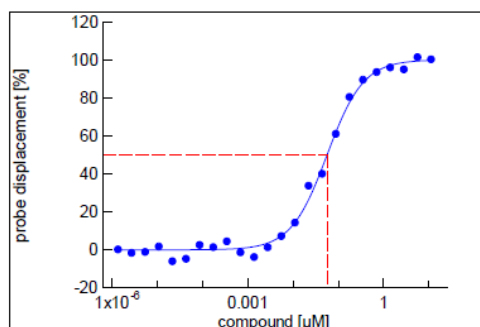


Figure S16. Kinetic binding data for compound 6a.



IC50:

time point [s]	IC50 [μM]	Kd [μM]
7294	5.64E-02	2.82E-02



secondary plot k_{obs} vs compound concentration:

k_{on} [1/s 1/μM]	k_{off} [1/s]	residence time [min]
2.17E-03	6.13E-05	272

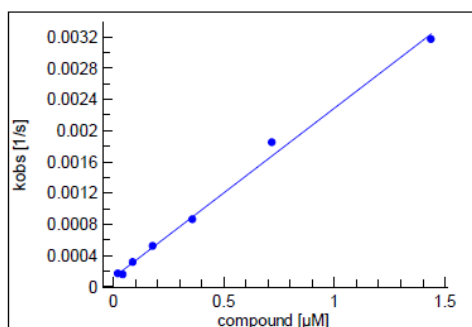
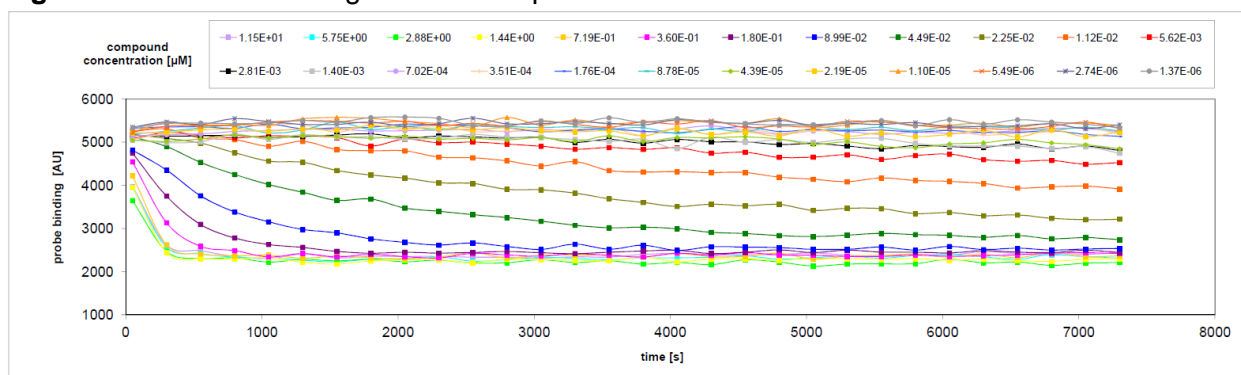


Figure S17. Kinetic binding data for compound 6b.



IC50:

time point [s]	IC50 [μM]	Kd [μM]
7299	1.01E-02	5.03E-03

secondary plot k_{obs} vs compound concentration:

kon [1/s 1/μM]	koff [1/s]	residence time [min]
1.41E-02	7.09E-05	235

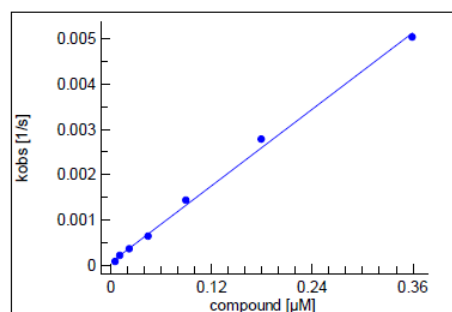
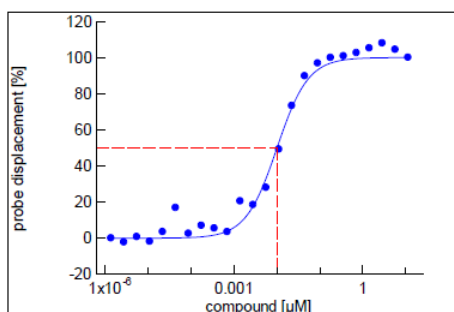
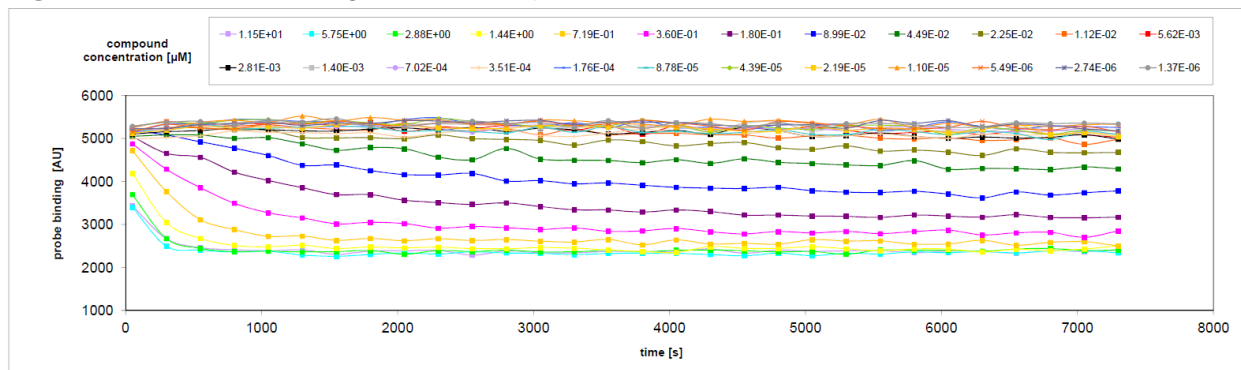


Figure S18. Kinetic binding data for compound 9.

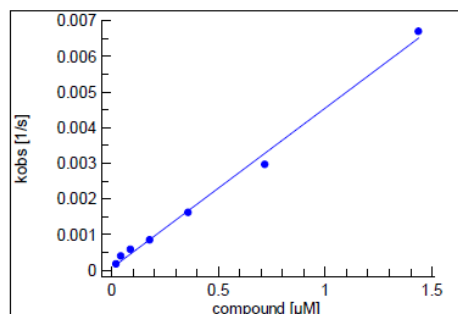
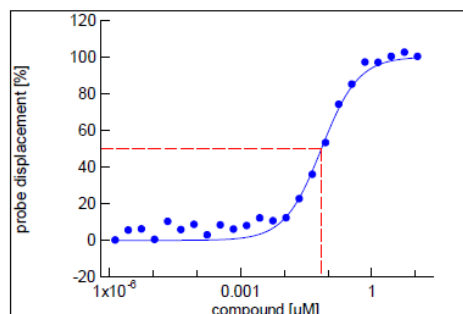


IC50:

time point [s]	IC50 [μM]	Kd [μM]
7299	7.09E-02	3.54E-02

secondary plot k_{obs} vs compound concentration:

kon [1/s 1/μM]	koff [1/s]	residence time [min]
4.49E-03	1.59E-04	105



Biochemical FGFR4 assay investigating the effect of inhibitor/FGFR4 preincubation times

Generation of the non-phosphorylated FGFR4 442-753 kinase domain protein was carried out as described in reference 4 in the main text. Assays were conducted in the same manner as described above for the 'standard screening conditions' except that the FGFR4 and inhibitor were preincubated for a period of 1, 2, 3, or 4 hours.

Concentration/inhibition curves are shown below, for single experiments, with selected compounds.

- Red curve** no preincubation
- Light green curve** 1 hour preincubation
- Blue curve** 2 hour preincubation
- Purple curve** 3 hour preincubation
- Dark green curve** 4 our preincubation

Figure S19. Effect of the preincubation time on the FGFR4 biochemical activity of compound 5.

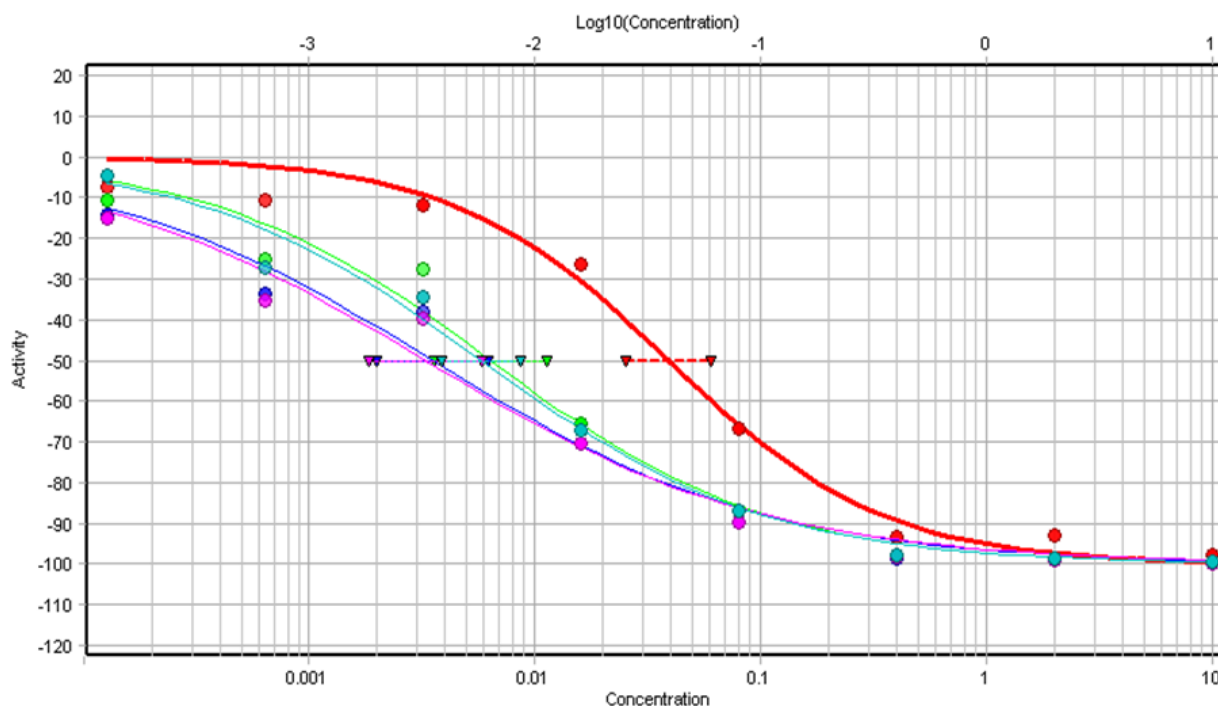


Figure S20. Effect of the preincubation time on the FGFR4 biochemical activity of compound **6a**.

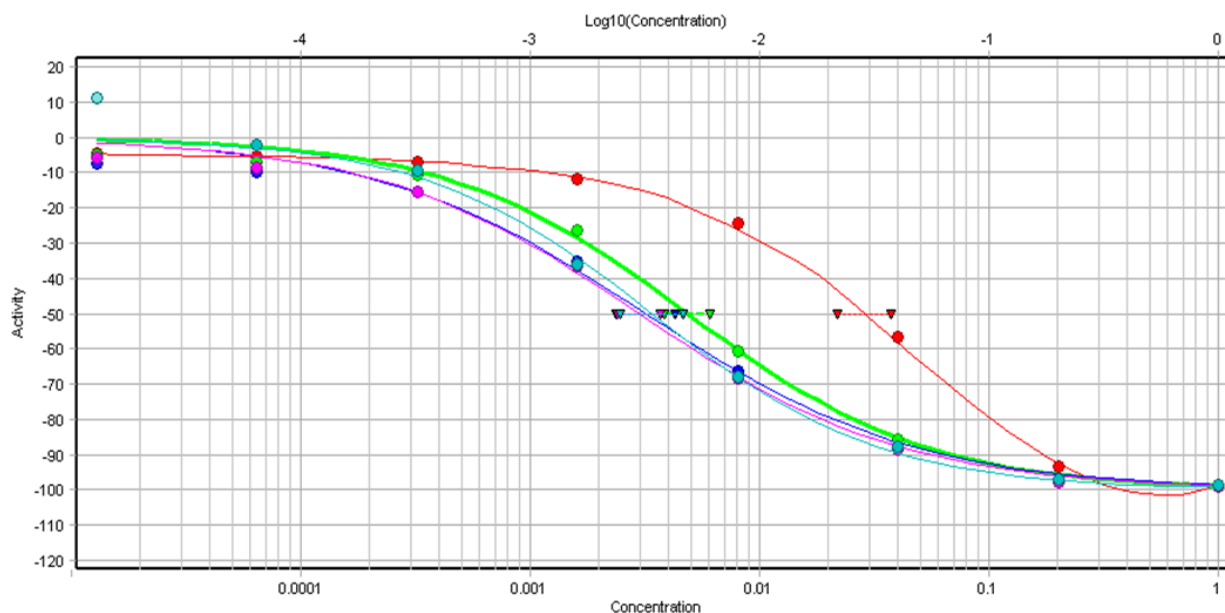


Table S5. The effect of preincubation time on FGFR4 biochemical activity.

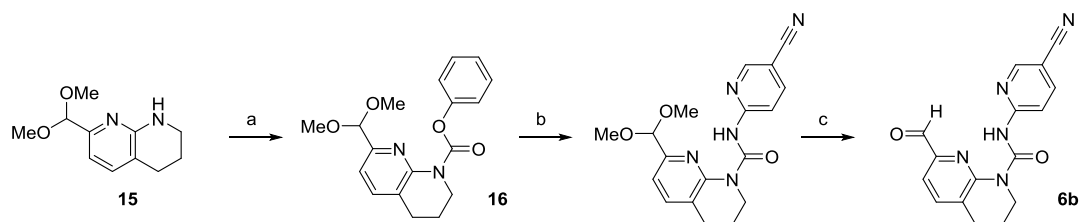
Compound	Biochemical IC ₅₀ values (nM)	
	no preincubation	1 h preincubation
1	1.5	1.3
5	84 ± 57	8.5 ± 1.1
6a	15 ± 3	4.2 ± 0.6
6b	6.8 ± 3.2	2.3 ± 1.1
6c	8.0	3.6
6d	200	140
6g	0.9	0.4
6j	33	6.8
7a	55	29
7f	16	18
7g	150	89
9	48	21
11a	830	510
11b	123 ± 9	13 ± 1
12a	4.9 ± 1.1	2.2
12b	5.2	1.0

data are from single experiments, or expressed as mean ± SD, where 2 to 7 repeated experiments were performed.

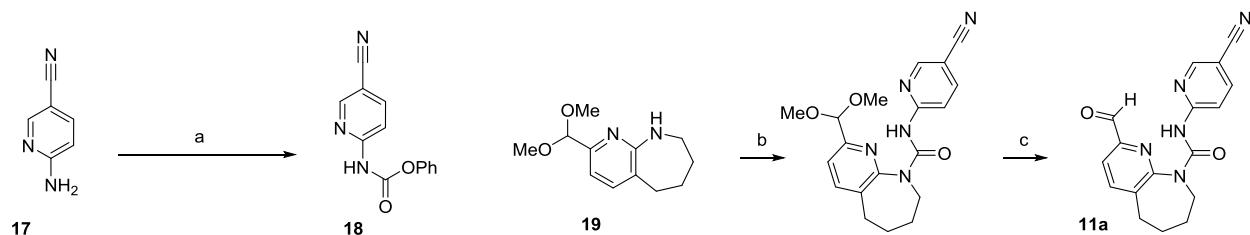
Compound synthesis

Solvents and reagents were purchased from suppliers and used without any further purification. Normal phase chromatography was conducted using a Teledyne ISCO, CombiFlash Rf system with silica gel pre-packed columns (RediSep® Rf). LC/MS was conducted using: Waters Acquity UPLC with Waters SQ detector; with a Acquity HSS T3 1.8 μm 2.1 x 50 mm column; eluting with gradients of aqueous acetonitrile containing formic acid and ammonium acetate modifiers. The purity of the final compounds was > 95% as judged by analysis of the AUC of the product peak (TAC, 210-450 nm) by LC/MS. Chemical shifts (δ) are reported in ppm relative to tetramethylsilane (TMS) and calibrated to the residual solvent proton peaks. The multiplicities of the signals are indicated as s-singlet, d-doublet, t-triplet, q-quartet, p-pentet, hept-heptet, m-multiplet, or br-broad. Coupling constants are quoted in Hz to one decimal place. Within this text, room temperature is defined as 19 – 25 °C.

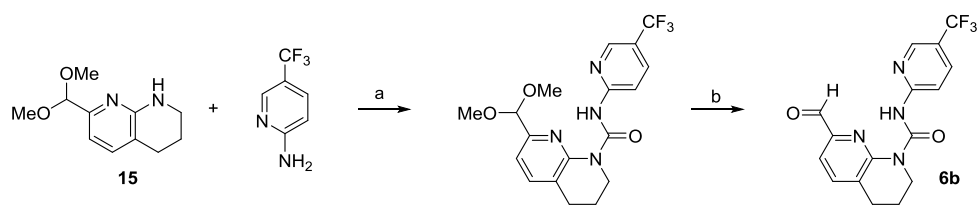
The synthetic sequences used to generate the analogues **6** to **12** and **14** are exemplified by the preparation of **6b**, **11a** and **6a** in Schemes S1 to S3. All starting materials used are commercially available.



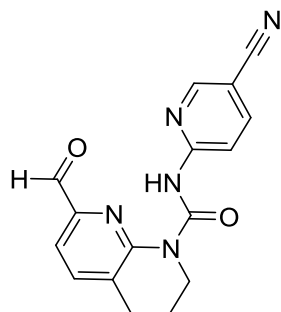
Scheme S1. Synthesis **6b**. Reagents and conditions: (a) LiHMDS, $(\text{PhO})_2\text{CO}$, THF, -15 °C, 0.5 h, 78%; (b) LiHMDS, 2-amino-5-cyanopyridine, THF, -15 °C, 25 min, 94%; (c) $\text{HCl}_{(\text{aq})}$, THF, 25 °C, 15 min, 96%.



Scheme S2. Synthesis of **11a**. Reagents and conditions: (a) $\text{PhO}(\text{CO})\text{Cl}$, pyridine, THF, 0-25 °C, 1.5 h, 84%; (b) **18**, DMAP, THF, reflux, 23 h, 54%; (c) conc. $\text{HCl}_{(\text{aq})}$, THF, 25 °C, 1 h, 76%.



Scheme S3. Synthesis of **6a**. Reagents and conditions: (a) COCl_2 (20% in toluene), NEt_3 , THF, 25 °C, 2.5 d, 36%; (b) conc. $\text{HCl}_{(\text{aq})}$, THF, then NMP, TFA, 25 °C, 5 h, 80%.



N-(5-cyanopyridin-2-yl)-7-formyl-3,4-dihydro-1,8-naphthyridine-1(2*H*)-carboxamide (**6b**).

Step 1: Phenyl 7-(dimethoxymethyl)-3,4-dihydro-1,8-naphthyridine-1(2*H*)-carboxylate (**16**).

A solution of 7-(dimethoxymethyl)-1,2,3,4-tetrahydro-1,8-naphthyridine (**15**, 2 g, 9.60 mmol) and diphenylcarbonate (4.11 g, 19.21 mmol) in THF (40 ml) at -15 °C was treated with LiHMDS (1 M in THF, 13.3 ml, 13.3 mmol) and stirred for 0.5 h. The reaction mixture was quenched with sat. aq. NH₄Cl and extracted with EtOAc (2x). The combined organic layers were washed with brine, dried over Na₂SO₄, filtered and concentrated under reduced pressure. The crude product was purified by normal phase chromatography (80 g silica gel cartridge, heptanes/EtOAc 100:0 to 25:75) to give 2.46 g (78%) of the title compound as a pale yellow solid.

¹H NMR (400 MHz, DMSO-*d*₆) δ 7.65 (d, *J* = 7.7 Hz, 1H), 7.46 - 7.38 (m, 2H), 7.27 - 7.18 (m, 4H), 5.17 (s, 1H), 3.87 - 3.80 (m, 2H), 3.26 (s, 6H), 2.83 (t, *J* = 6.5 Hz, 2H), 2.00 – 1.92 (m, 2H).

Step 2: *N*-(5-cyanopyridin-2-yl)-7-(dimethoxymethyl)-3,4-dihydro-1,8-naphthyridine-1(2*H*)-carboxamide.

A solution of phenyl 7-(dimethoxymethyl)-3,4-dihydro-1,8-naphthyridine-1(2*H*)-carboxylate (**16**, 262 mg, 0.798 mmol) and 2-amino-5-cyanopyridine (190 mg, 1.60 mmol) in THF (7.5 ml) at -15 °C under argon was treated dropwise with LiHMDS (1 M in THF, 1.60 ml, 1.60 mmol). The reaction mixture was stirred at -15 °C for 25 min and then quenched by addition of sat. aq. NH₄Cl and extracted with EtOAc (2x). The combined org. layers were washed with brine, dried over Na₂SO₄, filtered and concentrated under reduced pressure. The crude material was purified by normal phase chromatography (12 g silica gel cartridge, heptanes/EtOAc 100:0 to 0:100) to give 265 mg (94%) of the title compound as a white solid.

¹H NMR (400 MHz, DMSO-*d*₆) δ 13.90 (s, 1H), 8.78 (dd, *J* = 2.0, 1.2 Hz, 1H), 8.24 – 8.22 (m, 2H), 7.75 – 7.72 (m, 1H), 7.18 (d, *J* = 7.7 Hz, 1H), 5.37 (s, 1H), 3.99 – 3.92 (m, 2H), 3.37 (s, 6H), 2.85 (t, *J* = 6.3 Hz, 2H), 1.97 – 1.86 (m, 2H).

LCMS *m/z* calculated for C₁₈H₁₉N₅O₃: 353.15, found 354.1 [M+H].

Step 3. *N*-(5-cyanopyridin-2-yl)-7-formyl-3,4-dihydro-1,8-naphthyridine-1(2*H*)-carboxamide (**6b**).

A solution of *N*-(5-cyanopyridin-2-yl)-7-(dimethoxymethyl)-3,4-dihydro-1,8-naphthyridine-1(2*H*)-carboxamide (150 mg, 0.424 mmol) in THF (3 ml) was treated with water (2.25 ml) and HCl conc. (0.75 ml). The reaction mixture was stirred for 15 min at room temperature. The reaction was quenched by addition of sat. aq. NaHCO₃ (gas evolution) and extracted with DCM (3x). The combined organic layers were washed with brine, dried over Na₂SO₄, filtered and concentrated under reduced pressure. The crude material was purified by normal phase chromatography (12 g silica gel cartridge, heptanes/EtOAc 100:0 to 0:100) to give 125 mg (96%) of the title compound as a white solid.

¹H NMR (400 MHz, DMSO-*d*₆) δ 13.86 (s, 1H), 9.96 (d, *J* = 0.4 Hz, 1H), 8.80 (dd, *J* = 2.2, 0.9 Hz, 1H), 8.27 (dd, *J* = 8.8, 2.2 Hz 1H), 8.22 (dd, *J* = 8.8, 0.9 Hz 1H), 7.94 (d, *J* = 7.6 Hz, 1H), 7.68 (d, *J* = 7.6 Hz, 1H), 4.30 - 3.96 (m, 2H), 2.95 (t, *J* = 6.2 Hz, 2H), 2.03 - 1.90 (m, 2H).

¹³C NMR (100 MHz, DMSO-*d*₆) δ 190.6, 155.0, 152.4, 152.0, 151.4, 146.7, 142.0, 140.0, 129.4, 117.6, 117.4, 112.8, 102.9, 43.6, 27.7, 20.3.

LCMS *m/z* calculated for C₁₆H₁₃N₅O₂: 307.11, found 308.1 [M+H].

Figure S21. ¹H NMR of **6b**

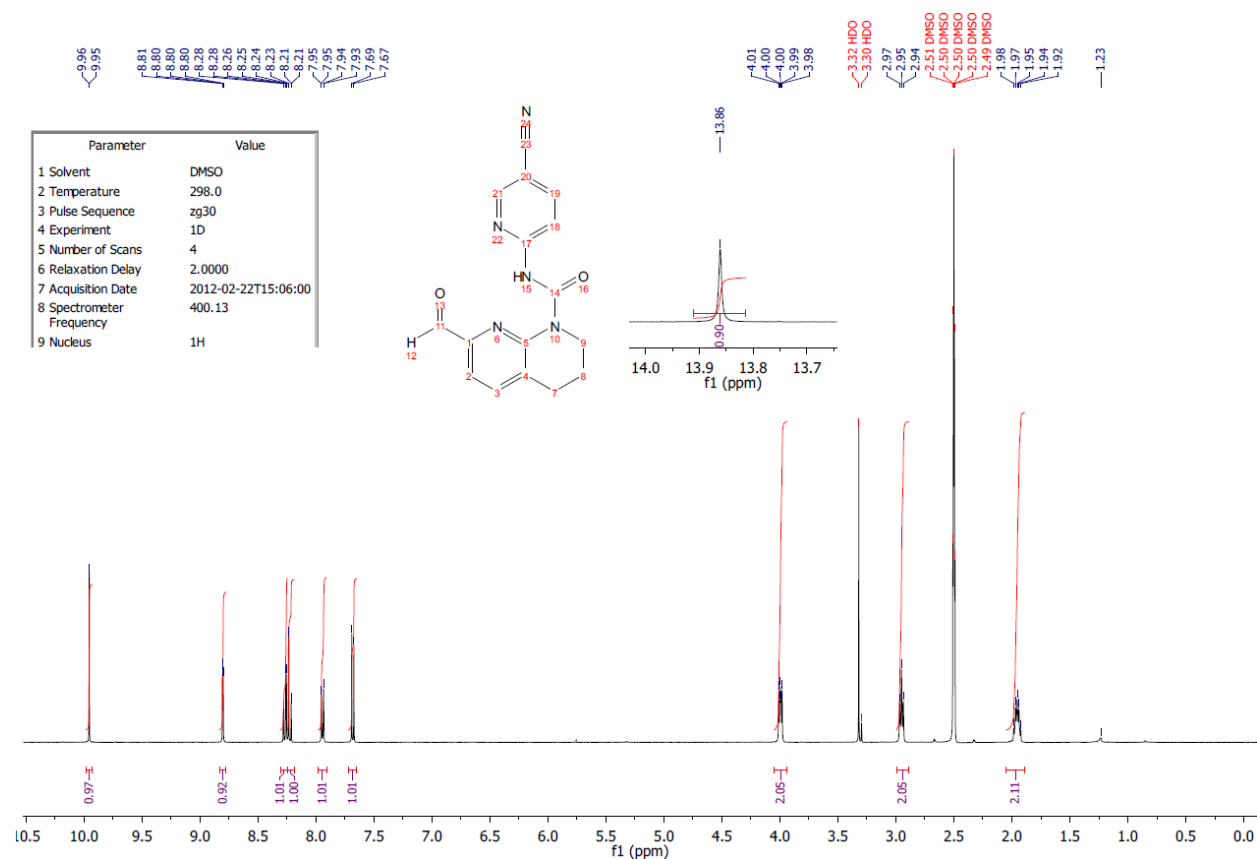


Figure S22. ^{13}C NMR of **6b**

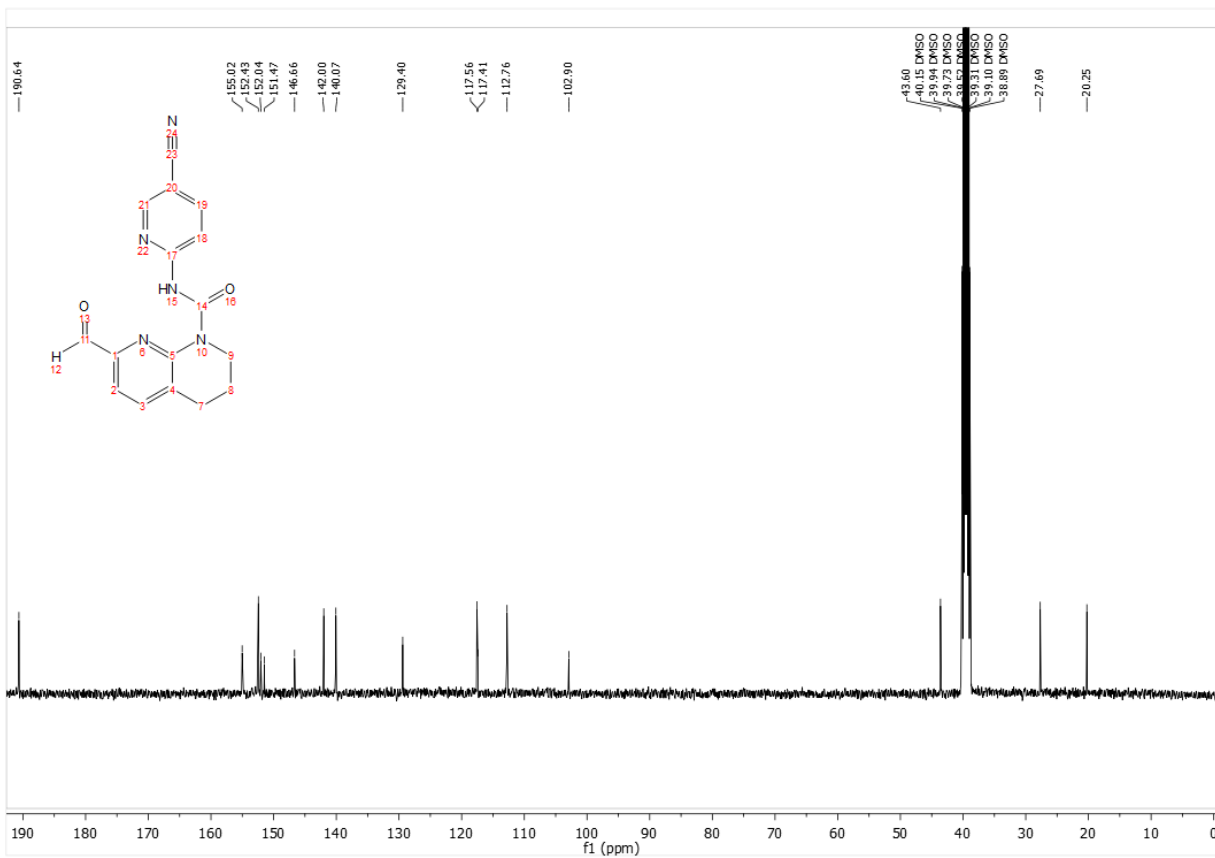
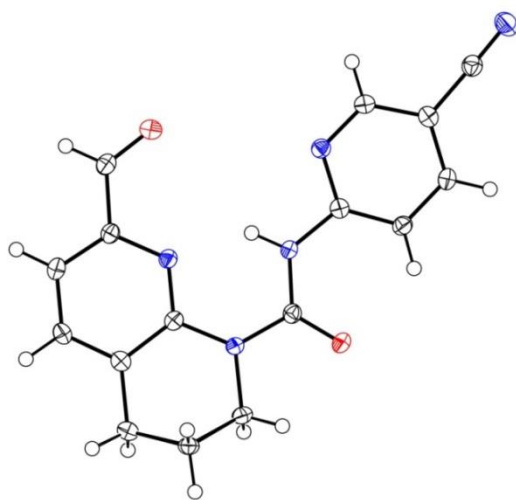
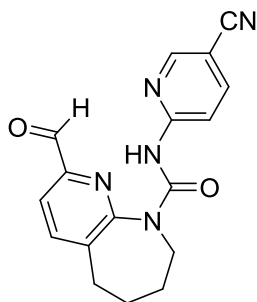


Figure S23. Crystallographic structure of **6b**



The structure of **6b** has been deposited in the Cambridge Structural Database CCDC 1585627 (www.ccdc.cam.ac.uk).



N-(5-cyanopyridin-2-yl)-2-formyl-5,6,7,8-tetrahydro-9*H*-pyrido[2,3-*b*]azepine-9-carboxamide (11a).

Step 1: phenyl (5-cyanopyridin-2-yl)carbamate (**18**).

Phenyl chloroformate (2.58 g, 16.3 mmol) was added dropwise to a mixture of 2-amino-5-cyanopyridine (2.0 g, 16.3 mmol) and pyridine (1.48 g, 18.7 mmol) in THF (40 ml) at 0 °C. The reaction mixture was stirred for 0.5 h at 0 °C and then 1 h at room temperature. The resulting suspension was filtered; the solid was washed with Et₂O (3x) and dried to give 3.29 g (84%) of the title compound as a light brown solid.

¹H NMR (600 MHz, DMSO-*d*₆) δ 11.38 (s, 1H), 8.81 (d, *J* = 2.3 Hz, 1H), 8.27 (dd, *J* = 8.8, 2.3 Hz, 1H), 7.97 (d, *J* = 8.8 Hz, 1H), 7.47 – 7.40 (m, 2H), 7.30 (t, *J* = 7.4 Hz, 1H), 7.27 – 7.22 (m, 2H).

LCMS *m/z* calculated for C₁₃H₉N₃O₂: 239.07, found 240.0 [M+H].

Step 2: *N*-(5-cyanopyridin-2-yl)-2-(dimethoxymethyl)-7,8-dihydro-5*H*-pyrido[2,3-*b*]azepine-9(6*H*)-carboxamide.

A mixture of 2-(dimethoxymethyl)-6,7,8,9-tetrahydro-5*H*-pyrido[2,3-*b*]azepine (**19**, 35 mg, 0.154 mmol), phenyl (5-cyanopyridin-2-yl)carbamate (**18**, 122 mg, 0.509 mmol) and DMAP (28.3 mg, 0.231 mmol) in THF (1.7 ml) was heated at reflux for 23 h. The reaction mixture was diluted with sat. aq. NaHCO₃ and extracted with DCM (3x). The combined organic layers were dried over Na₂SO₄ and evaporated. The crude material was applied to a 40 g RediSep® silica column and purified by normal phase chromatography, eluting with 99:1 DCM/MeOH. Product-containing fractions were combined and evaporated. The residue was triturated with Et₂O and the solid removed by filtration. The filtrate was concentrated and the residue triturated with MeOH to give 30.5 mg (54%) of the title compound as a white solid.

¹H NMR (600 MHz, DMSO-*d*₆) δ 10.12 (br s, 1H), 8.65 (s, 1H), 8.22 – 8.14 (m, 1H), 8.10 – 8.03 (m, 1H), 7.84 (d, *J* = 7.7 Hz, 1H), 7.36 (d, *J* = 7.7 Hz, 1H), 5.27 (s, 1H), 3.93 – 3.49 (m, 2H), 3.30 (s, 6H), 2.82 (t, *J* = 5.8 Hz, 2H), 1.87 – 1.75 (m, 2H), 1.75 – 1.65 (m, 2H).

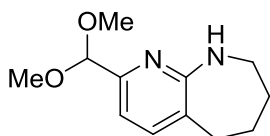
LCMS *m/z* calculated for C₁₉H₂₁N₅O₃: 367.16, found 368.1 [M+H].

Step 3: *N*-(5-cyanopyridin-2-yl)-2-formyl-5,6,7,8-tetrahydro-9*H*-pyrido[2,3-*b*]azepine-9-carboxamide (**11a**).

Concentrated hydrochloric acid (0.65 ml) was added to a solution of *N*-(5-cyanopyridin-2-yl)-2-(dimethoxymethyl)-7,8-dihydro-5*H*-pyrido[2,3-*b*]azepine-9(6*H*)-carboxamide (29 mg, 0.079 mmol) in THF (0.9 ml) at room temperature. After stirring for 1 h at room temperature, sat. aq. NaHCO₃ was added and the mixture extracted with DCM (3x). The combined organic layers were washed with brine, dried over Na₂SO₄ and evaporated. The residue was triturated with Et₂O to give 19.4 mg (76%) of the title compound as a white solid.

¹H NMR (400 MHz, DMSO-*d*₆) δ 10.00 (br s, 1H), 9.88 (s, 1H), 8.67 (m, 1H), 8.20 (m, 1H), 8.11 (d, *J* = 8.9 Hz, 1H), 8.04 (d, *J* = 7.7 Hz, 1H), 7.84 (s, 1H), 3.73 (m, 2H), 2.91 (m, 2H), 1.82 (m, 2H), 1.72 (m, 2H).

LCMS *m/z* calculated for C₁₇H₁₅N₅O₂: 321.12, found 322.1 [M+H].



2-(dimethoxymethyl)-6,7,8,9-tetrahydro-5*H*-pyrido[2,3-*b*]azepine (**19**).

Step 1: tert-butyl 2-vinyl-7,8-dihydro-5*H*-pyrido[2,3-*b*]azepine-9(6*H*)-carboxylate.

A degassed mixture of tert-butyl 2-chloro-7,8-dihydro-5*H*-pyrido[2,3-*b*]azepine-9(6*H*)-carboxylate (690 mg, 2.44 mmol), potassium trifluoro(vinyl)borate (344 mg, 2.44 mmol), PdCl₂(dppf).CH₂Cl₂ (199 mg, 0.244 mmol) and Cs₂CO₃ (2.00 g, 6.1 mmol) in THF (50 ml) and H₂O (10 ml) was heated at 80 °C for 3.5 h. The reaction mixture was diluted with H₂O and extracted with DCM (2x). The combined organic layers were dried over Na₂SO₄ and evaporated. The crude material was applied to a 120 g RediSep® silica column and purified by normal phase chromatography, eluting with 1:3 EtOAc/heptanes. Product-containing fractions were combined and evaporated to give 472 mg (68%) of the title compound as an off-white solid.

LCMS *m/z* calculated for C₁₆H₂₂N₂O₂: 274.17, found 275.2 [M+H].

Step 2: tert-butyl 2-formyl-7,8-dihydro-5*H*-pyrido[2,3-*b*]azepine-9(6*H*)-carboxylate.

Ozone was bubbled through a mixture of tert-butyl 2-vinyl-7,8-dihydro-5*H*-pyrido[2,3-*b*]azepine-9(6*H*)-carboxylate (470 mg, 1.66 mmol) in DCM (6.5 ml) at -78 °C. After 15 minutes, the intermediate ozonide was treated with dimethyl sulfide (0.86 ml, 11.62 mmol) and then the reaction mixture was slowly warmed to room temperature. After 1.5 h, the mixture was diluted with H₂O and extracted with DCM (3x). The combined organic layers were washed with sat. aq. NaHCO₃ and brine, dried over Na₂SO₄ and evaporated to give 416 mg of the crude title compound as a light brown solid. This material was used without purification in the next reaction.

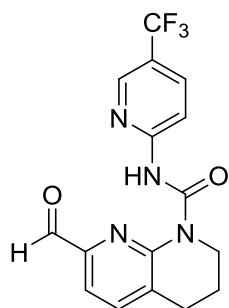
LCMS *m/z* calculated for C₁₅H₂₀N₂O₃: 276.15, found 277.1 [M+H].

Step 3: 2-(dimethoxymethyl)-6,7,8,9-tetrahydro-5*H*-pyrido[2,3-*b*]azepine.

A microwave vial was charged with a mixture of tert-butyl 2-formyl-7,8-dihydro-5*H*-pyrido[2,3-*b*]azepine-9(6*H*)-carboxylate (415 mg, 1.277 mmol) and *p*-toluenesulfonic acid monohydrate (110 mg, 0.573 mmol) in MeOH (64 ml), sealed and then heated at 135 °C for 3.5 h. The reaction mixture was concentrated and the residue partitioned between sat. aq. NaHCO₃ and EtOAc. The aq. phase was extracted with EtOAc (2x) - the combined organic layers were dried over Na₂SO₄ and evaporated. The crude material was applied to a 120 g RediSep® silica column and purified by normal phase chromatography, eluting with EtOAc. Product-containing fractions were combined and evaporated to give 150 mg (39% over two steps) of the title compound as a light yellow oil.

¹H NMR (600 MHz, DMSO-*d*₆) δ 7.37 (d, *J* = 7.5 Hz, 1H), 6.73 (d, *J* = 7.5 Hz, 1H), 5.93 (t, *J* = 4.0 Hz, 1H), 5.05 (s, 1H), 3.24 (s, 6H), 3.07 – 3.00 (m, 2H), 2.67 – 2.60 (m, 2H), 1.71 – 1.66 (m, 2H), 1.66 – 1.60 (m, 2H).

LCMS *m/z* calculated for C₁₂H₁₈N₂O₂: 222.14, found 223.1 [M+H].



7-formyl-N-(5-(trifluoromethyl)pyridin-2-yl)-3,4-dihydro-1,8-naphthyridine-1(2*H*)-carboxamide (6a)

Step 1: 7-(dimethoxymethyl)-N-(5-(trifluoromethyl)pyridin-2-yl)-3,4-dihydro-1,8-naphthyridine-1(2*H*)-carboxamide.

To a solution of phosgene (20% solution in toluene, 0.265 ml, 0.504 mmol) in THF (2 ml) was added triethylamine (0.20 ml, 1.44 mmol). Subsequently, a solution of 7-(dimethoxymethyl)-1,2,3,4-tetrahydro-1,8-naphthyridine (intermediate 4, 100 mg, 0.480 mmol) in THF (2 ml) was added drop wise. The resulting yellow suspension was stirred for 15 min, then 5-(trifluoromethyl)pyridin-2-amine (93 mg, 0.576 mmol) was added and the reaction mixture stirred for 2.5 days. The reaction mixture was diluted with sat. aq. NaHCO₃ and extracted twice with EtOAc. The combined organic layers were dried over Na₂SO₄, filtered and concentrated under reduced pressure. The crude material was purified by normal phase chromatography (12 g silica

gel cartridge, heptanes/EtOAc 100:0 to 0:100). The product containing fractions were concentrated to give 67.6 mg (36%) of the title compound as a white solid.

^1H NMR (400 MHz, DMSO- d_6) δ 13.83 (s, 1H), 8.70 (s, 1H), 8.26 (d, J = 8.9 Hz, 1H), 8.20 - 8.12 (m, 1H), 7.73 (d, J = 7.7 Hz, 1H), 7.18 (d, J = 7.7 Hz, 1H), 5.37 (s, 1H), 4.01 - 3.93 (m, 2H), 3.39 (s, 6H), 2.86 (t, J = 6.3 Hz, 2H), 1.98 - 1.87 (m, 2H).

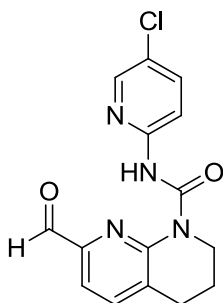
LCMS m/z calculated for $\text{C}_{18}\text{H}_{19}\text{F}_3\text{N}_4\text{O}_3$: 396.14, found 397.0 [M+H].

Step 2: 7-formyl-*N*-(5-(trifluoromethyl)pyridin-2-yl)-3,4-dihydro-1,8-naphthyridine-1(2*H*)-carboxamide (**6a**).

A solution of 7-(dimethoxymethyl)-*N*-(5-(trifluoromethyl)pyridin-2-yl)-3,4-dihydro-1,8-naphthyridine-1(2*H*)-carboxamide (64.5 mg, 0.163 mmol) in THF (0.4 ml) at room temperature was treated with water (0.6 ml) and conc. HCl (0.20 ml). After the addition, additional THF (0.2 ml) was added and the reaction mixture was stirred at room temperature for 2.5 h. Subsequently, NMP (0.1 ml) was added followed by TFA (0.10 ml, 1.3 mmol) and the resulting solution was stirred for 2 h. The reaction was then quenched by the addition of sat. aq. NaHCO_3 (gas evolution) and extracted with EtOAc (2x). The combined organic layers were washed with brine, dried over anhydrous Na_2SO_4 , filtered and concentrated under reduced pressure. The crude material was purified by normal phase chromatography (12 g silica gel cartridge, heptanes/EtOAc 100:0 to 0:100) to give 45.7 mg (80%) of the title compound as a white solid.

^1H NMR (400 MHz, DMSO- d_6) δ 13.78 (s, 1H), 9.97 (s, 1H), 8.76 – 8.70 (m, 1H), 8.28 (d, J = 8.9 Hz, 1H), 8.20 (dd, J = 8.9, 2.5 Hz, 1H), 7.94 (d, J = 7.5 Hz, 1H), 7.68 (d, J = 7.5 Hz, 1H), 4.05 – 3.97 (m, 2H), 2.96 (t, J = 6.3 Hz, 2H), 2.02 - 1.91 (m, 2H).

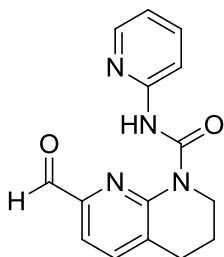
LCMS m/z calculated for $\text{C}_{16}\text{H}_{13}\text{F}_3\text{N}_4\text{O}_2$: 350.10, found 351.0 [M+H].



N-(5-chloropyridin-2-yl)-7-formyl-3,4-dihydro-1,8-naphthyridine-1(2*H*)-carboxamide (**6c**) was prepared according to S3 using 7-(dimethoxymethyl)-1,2,3,4-tetrahydro-1,8-naphthyridine (**15**) and 5-chloropyridin-2-amine.

^1H NMR (400 MHz, $\text{DMSO-}d_6$) δ 13.54 (s, 1H), 9.95 (s, 1H), 8.38 (d, $J = 2.5$ Hz, 1H), 8.11 (d, $J = 8.9$ Hz, 1H), 7.92 (dd, $J = 8.9, 2.5$ Hz, 2H), 7.66 (d, $J = 7.5$ Hz, 1H), 4.03 - 3.96 (m, 2H), 2.95 (t, $J = 6.3$ Hz, 2H), 1.90 - 1.99 (m, 2H).

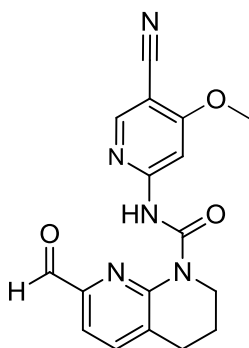
LCMS m/z calculated for $\text{C}_{15}\text{H}_{13}\text{ClN}_4\text{O}_2$: 316.07, found 317.0 [M+H].



7-formyl-*N*-(pyridin-2-yl)-3,4-dihydro-1,8-naphthyridine-1(2*H*)-carboxamide (6d) was prepared according to S3 using 7-(dimethoxymethyl)-1,2,3,4-tetrahydro-1,8-naphthyridine (**15**) and pyridine-2-amine.

^1H NMR (400 MHz, $\text{DMSO-}d_6$) δ 13.49 (s, 1H), 9.97 (s, 1H), 8.35 (dd, $J = 4.9, 1.9$ Hz, 1H), 8.07 (d, $J = 8.4$ Hz, 1H), 7.92 (d, $J = 7.5$ Hz, 1H), 7.88 - 7.79 (m, 1H), 7.66 (d, $J = 7.5$ Hz, 1H), 7.11 (dd, $J = 6.3, 4.9$ Hz, 1H), 4.04 - 3.96 (m, 2H), 2.95 (t, $J = 6.2$ Hz, 2H), 2.00 - 1.89 (m, 2H).

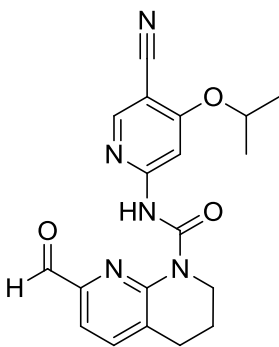
LCMS m/z calculated for $\text{C}_{15}\text{H}_{14}\text{N}_4\text{O}_2$: 282.11, found 283.1 [M+H].



N-(5-cyano-4-methoxypyridin-2-yl)-7-formyl-3,4-dihydro-1,8-naphthyridine-1(2*H*)-carboxamide (6e) was prepared according to S1 using 7-(dimethoxymethyl)-1,2,3,4-tetrahydro-1,8-naphthyridine (**15**) and 6-amino-4-methoxynicotinonitrile.

^1H NMR (400 MHz, $\text{DMSO-}d_6$) δ 13.84 (s, 1H), 9.94 (s, 1H), 8.60 (s, 1H), 7.91 - 7.98 (m, 2H), 7.68 (d, $J = 7.5$ Hz, 1H), 3.97 - 4.03 (m, 5H), 2.95 (t, $J = 6.3$ Hz, 2H), 1.91 - 2.00 (m, 2H).

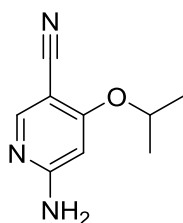
LCMS m/z calculated for $\text{C}_{17}\text{H}_{15}\text{N}_5\text{O}_3$: 337.12, found 338.4 [M+H].



N-(5-cyano-4-isopropoxy-pyridin-2-yl)-7-formyl-3,4-dihydro-1,8-naphthyridine-1(2*H*)-carboxamide (6f) was prepared according to S1 using 7-(dimethoxymethyl)-1,2,3,4-tetrahydro-1,8-naphthyridine (**15**) and 6-amino-4-isopropoxynicotinonitrile.

¹H NMR (400 MHz, chloroform-*d*) δ 13.87 (br. s., 1 H), 10.14 (s, 1 H), 8.39 (s, 1 H), 7.96 (s, 1 H), 7.62 - 7.74 (m, 2 H), 4.82 - 4.92 (m, 1 H), 4.08 - 4.16 (m, 2 H), 2.98 (t, *J* = 6.3 Hz, 2 H), 2.03 - 2.13 (m, 2 H), 1.47 (d, *J* = 6.0 Hz, 6 H).

LCMS *m/z* calculated for C₁₉H₁₉N₅O₃: 365.15, found 366.2 [M+H].

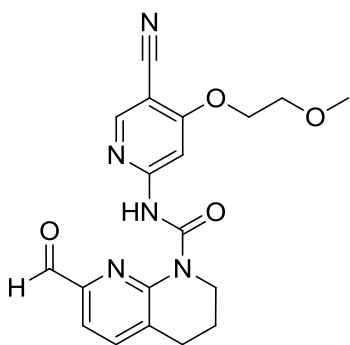


6-amino-4-isopropoxynicotinonitrile.

KHMDS (87 g, 438 mmol) was added portion wise to a solution of propan-2-ol (26.3 g, 438 mmol) in THF (250 ml) at room temperature. After 15 min a solution of 6-amino-4-fluoronicotinonitrile (30 g, 219 mmol) in THF (200 ml) was added and the reaction mixture stirred for 18 h at room temperature. The reaction mixture was partitioned between saturated aqueous NH₄Cl and EtOAc, extracted with EtOAc (2x), the combined EtOAc layers were dried over Na₂SO₄ and evaporated. The residue was triturated with Et₂O and 24.4 g (62%) of the product obtained by filtration as a yellow solid.

¹H NMR (400 MHz, DMSO-*d*₆) δ 8.12 (s, 1H), 6.82 (s, 2H), 6.07 (s, 1H), 4.64 (septet, *J* = 6.2 Hz 1H), 1.31 (d, *J* = 6.2 Hz, 6H).

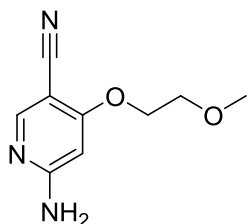
LCMS *m/z* calculated for C₉H₁₁N₃O: 177.09, found 178.1 [M+H].



N-(5-cyano-4-(2-methoxyethoxy)pyridin-2-yl)-7-formyl-3,4-dihydro-1,8-naphthyridine-1(2*H*)-carboxamide (6g) was prepared according to S1 using 7-(dimethoxymethyl)-1,2,3,4-tetrahydro-1,8-naphthyridine (**15**) and 6-amino-4-(2-methoxyethoxy)nicotinonitrile.

^1H NMR (400 MHz, DMSO- d_6) δ 13.81 (s, 1H), 9.95 (s, 1H), 8.60 (s, 1H), 7.97 – 7.92 (m, 2H), 7.68 (d, J = 7.5 Hz, 1H), 4.38 – 4.33 (m, 2H), 4.02 – 3.97 (m, 2H), 3.78 – 3.72 (m, 2H), 3.35 (s, 3H), 2.95 (t, J = 6.3 Hz, 2H), 2.00 – 1.92 (m, 2H).

LCMS m/z calculated for $\text{C}_{19}\text{H}_{19}\text{N}_5\text{O}_4$: 381.14, found 382.1 [M+H].

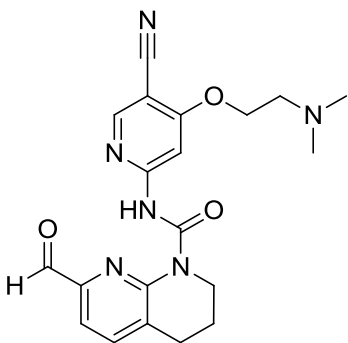


6-amino-4-(2-methoxyethoxy)nicotinonitrile.

A solution of KHMDS in THF (1 M, 48.1 ml, 48.1 mmol) was added to a solution of 2-methoxy ethanol (1.68 g, 21.88 mmol) in THF (90 ml) at room temperature. After 2 minutes, 6-amino-4-fluoronicotinonitrile (3.00 g, 21.9 mmol) was added and the reaction mixture stirred for 16 h at room temperature. The reaction mixture was partitioned between saturated aqueous NH_4Cl and EtOAc, extracted with EtOAc (2x), the combined EtOAc layers were washed with brine, dried over MgSO_4 and evaporated. The residue was triturated with EtOAc and 3.45 g (80%) of the title compound obtained by filtration as a beige solid.

^1H NMR (400 MHz, DMSO- d_6) δ 8.14 (s, 1H), 6.91 (s, br, 2H), 6.03 (s, 1H), 4.19 – 4.13 (m, 2H), 3.34 – 3.28 (m, 2H), 2.51 (s, 3H).

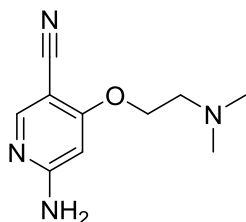
LCMS m/z calculated for $\text{C}_9\text{H}_{11}\text{N}_3\text{O}_2$: 193.09, found 194.1 [M+H].



N-(5-cyano-4-(2-(dimethylamino)ethoxy)pyridin-2-yl)-7-formyl-3,4-dihydro-1,8-naphthyridine-1(2*H*)-carboxamide (6h) was prepared according to S1 using 7-(dimethoxymethyl)-1,2,3,4-tetrahydro-1,8-naphthyridine (**15**) and 6-amino-4-(2-(dimethylamino)ethoxy)nicotinonitrile.

¹H NMR (400 MHz, DMSO-*d*₆) δ 13.82 (s, 1H), 9.95 (s, 1H), 8.59 (s, 1H), 7.92 - 7.97 (m, 2H), 7.68 (d, *J* = 7.5 Hz, 1H), 4.30 (t, *J* = 5.5 Hz, 2H), 3.97 - 4.03 (m, 2H), 2.95 (t, *J* = 6.3 Hz, 2H), 2.72 (t, *J* = 5.5 Hz, 2H), 2.25 (s, 6H), 1.90 - 2.00 (m, 2H).

LCMS *m/z* calculated for C₂₀H₂₂N₆O₃: 394.18, found 395.2 [M+H].

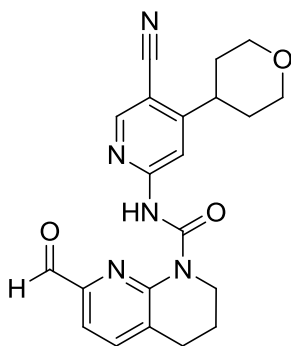


6-amino-4-(2-(dimethylamino)ethoxy)nicotinonitrile.

2-(dimethylamino)ethanol (0.293 ml, 2.92 mmol) was treated at room temperature with KHMDS (1 M in THF, 2.19 ml, 2.19 mmol). The reaction mixture was stirred for 2 min and then added to a solution of 6-amino-4-fluoronicotinonitrile (100 mg, 0.729 mmol) in THF (2 ml). The resulting dark brown solution was stirred at room temperature for 60 min, quenched with sat. aq. NH₄Cl, directly absorbed on isolate and dried under vacuum. The crude material was purified by reverse phase chromatography (13 g C18 cartridge, 0.1% TFA in water/acetonitrile 100:0 to 0:100). The product containing fractions were concentrated. The residue was treated with a small amount sat. aq. NaHCO₃ and NaCl (s) and extracted with CH₂Cl₂ (5x). The combined organic layers were dried over Na₂SO₄ and concentrated to give 62.4 mg (39%) the title compound as a white solid.

¹H NMR (400 MHz, DMSO-*d*₆) δ 8.14 (s, 1H), 6.89 (s, br, 2H), 6.05 (s, 1H), 4.12 (t, *J* = 5.8 Hz, 2H), 2.66 (t, *J* = 5.8 Hz, 2H), 2.23 (s, 6H).

LCMS *m/z* calculated for C₁₀H₁₄N₄O: 206.12, found 207.2 [M+H].



N-(5-cyano-4-(tetrahydro-2*H*-pyran-4-yl)pyridin-2-yl)-7-formyl-3,4-dihydro-1,8-naphthyridine-1(2*H*)-carboxamide (**6i**).

Step 1: *N*-(4-chloro-5-cyanopyridin-2-yl)-7-(dimethoxymethyl)-3,4-dihydro-1,8-naphthyridine-1(2*H*)-carboxamide. *N*-(4-chloro-5-cyanopyridin-2-yl)-7-(dimethoxymethyl)-3,4-dihydro-1,8-naphthyridine-1(2*H*)-carboxamide was prepared according to S1 using 7-(dimethoxymethyl)-1,2,3,4-tetrahydro-1,8-naphthyridine (**15**) and 6-amino-4-chloronicotinonitrile.

LCMS *m/z* calculated for C₁₈H₁₈ClN₅O₃: 387.11, found 388.1 [M+H].

Step 2: *N*-(5-cyano-4-(3,6-dihydro-2*H*-pyran-4-yl)pyridin-2-yl)-7-(dimethoxymethyl)-3,4-dihydro-1,8-naphthyridine-1(2*H*)-carboxamide.

N-(4-chloro-5-cyanopyridin-2-yl)-7-(dimethoxymethyl)-3,4-dihydro-1,8-naphthyridine-1(2*H*)-carboxamide (60 mg, 0.155 mmol), 2-(3,6-dihydro-2*H*-pyran-4-yl)-4,4,5,5-tetramethyl-1,3,2-dioxaborolane (65.0 mg, 0.309 mmol), PdCl₂(PPh₃)₂ (10.9 mg, 0.015 mmol), Na₂CO₃ (2 M in water, 0.232 ml, 0.464 mmol) and DME (2 ml) were charged into a sealed vial under argon. The mixture was stirred at 100 °C for 1 h, cooled to room temperature, diluted in EtOAc and washed with sat. aq. NaHCO₃ (2x) and brine. The organic layer was dried over Na₂SO₄, filtered and concentrated under vacuum. The crude material was purified by normal phase chromatography (4 g silica gel cartridge, heptanes/EtOAc 100:0 to 0:100) the product fractions were concentrated to give 41.2 mg (58%) of the title compound as a white solid.

LCMS *m/z* calculated for C₂₃H₂₅N₅O₄: 435.19, found 436.2 [M+H].

Step 3: *N*-(5-cyano-4-(tetrahydro-2*H*-pyran-4-yl)pyridin-2-yl)-7-(dimethoxymethyl)-3,4-dihydro-1,8-naphthyridine-1(2*H*)-carboxamide.

N-(5-cyano-4-(3,6-dihydro-2*H*-pyran-4-yl)pyridin-2-yl)-7-(dimethoxymethyl)-3,4-dihydro-1,8-naphthyridine-1(2*H*)-carboxamide (35 mg, 0.080 mmol) was dissolved in MeOH (1 ml) and THF (3 ml). The solution was treated with palladium (10% on charcoal, 8.55 mg, 8.04 μmol) and stirred under a H₂ atmosphere at room temperature for 16 h. The reaction mixture was filtered

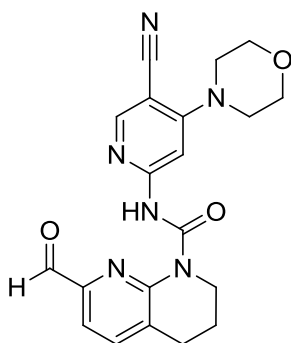
through a celite plug. The plug was rinsed with EtOAc and the filtrate was concentrated under vacuum. The residue was purified by normal phase chromatography (4 g silica gel cartridge, heptanes/EtOAc 100:0 to 0:100) to give 23.6 mg (64%) of the title compound as a white solid.

LCMS m/z calculated for $C_{23}H_{27}N_5O_4$: 437.21, found 438.2 [M+H].

Step 4: *N*-(5-cyano-4-(tetrahydro-2*H*-pyran-4-yl)pyridin-2-yl)-7-formyl-3,4-dihydro-1,8-naphthyridine-1(2*H*)-carboxamide (**6i**) was prepared according to S1 using *N*-(5-cyano-4-(tetrahydro-2*H*-pyran-4-yl)pyridin-2-yl)-7-(dimethoxymethyl)-3,4-dihydro-1,8-naphthyridine-1(2*H*)-carboxamide.

1H NMR (400 MHz, DMSO- d_6) δ 13.84 (s, 1H), 9.95 (s, 1H), 8.74 (s, 1H), 8.23 (s, 1H), 7.95 (d, J = 7.5 Hz, 1H), 7.68 (d, J = 7.5 Hz, 1H), 3.97 - 4.04 (m, 4H), 3.44 - 3.54 (m, 2H), 3.04 - 3.14 (m, 1H), 2.95 (t, J = 6.3 Hz, 2H), 1.92 - 1.98 (m, 2H), 1.65 - 1.84 (m, 4H).

LCMS m/z calculated for $C_{21}H_{21}N_5O_3$: 391.16, found 392.2 [M+H].



N-(5-cyano-4-morpholinopyridin-2-yl)-7-formyl-3,4-dihydro-1,8-naphthyridine-1(2*H*)-carboxamide (**6j**).

Step 1: *N*-(5-cyano-4-morpholinopyridin-2-yl)-7-(dimethoxymethyl)-3,4-dihydro-1,8-naphthyridine-1(2*H*)-carboxamide.

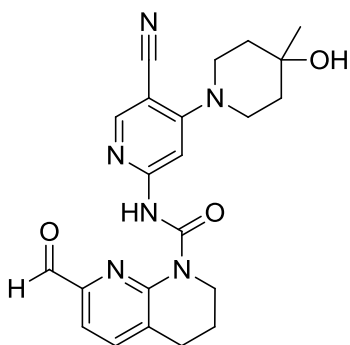
N-(4-chloro-5-cyanopyridin-2-yl)-7-(dimethoxymethyl)-3,4-dihydro-1,8-naphthyridine-1(2*H*)-carboxamide (60 mg, 0.155 mmol) and morpholine (500 μ l, 5.74 mmol) were dissolved in DMA (1 ml) under argon. The mixture was stirred at 100 $^{\circ}C$ for 1 h. The reaction mixture was cooled to room temperature, diluted in EtOAc and washed 2x with NH_4Cl aq sat and 1x with brine. The combined organic layers were dried over Na_2SO_4 , filtered and concentrated under reduced pressure. The crude material was purified by normal phase chromatography (4 g silica gel cartridge, heptanes/EtOAc 100:0 to 0:100) followed by reverse phase chromatography (4.3 g C18 cartridge, 0.1% TFA in water/acetonitrile 90:10 to 0:100) to give 32 mg (45%) of the title compound as a white solid.

LCMS m/z calculated for C₂₂H₂₆N₆O₄: 438.20, found 439.2 [M+H].

Step 2: *N*-(5-cyano-4-morpholinopyridin-2-yl)-7-formyl-3,4-dihydro-1,8-naphthyridine-1(2*H*)-carboxamide (**6j**). *N*-(5-cyano-4-morpholinopyridin-2-yl)-7-formyl-3,4-dihydro-1,8-naphthyridine-1(2*H*)-carboxamide (**6j**) was prepared according to S1 using *N*-(5-cyano-4-morpholinopyridin-2-yl)-7-(dimethoxymethyl)-3,4-dihydro-1,8-naphthyridine-1(2*H*)-carboxamide.

¹H NMR (400 MHz, DMSO-*d*₆) δ ppm 13.65 (s, 1H), 9.93 (s, 1H), 8.48 (s, 1H), 7.93 (d, *J* = 7.5 Hz, 1H), 7.78 (s, 1H), 7.66 (d, *J* = 7.5 Hz, 1H), 3.96 - 4.01 (m, 2H), 3.74 - 3.80 (m, 4H), 3.40 - 3.46 (m, 4H), 2.95 (t, *J* = 6.3 Hz, 2H), 1.89 - 1.99 (m, 2H).

LCMS m/z calculated for C₂₀H₂₀N₆O₃: 392.16, found 393.1 [M+H].



N-(5-cyano-4-(4-hydroxy-4-methylpiperidin-1-yl)pyridin-2-yl)-7-formyl-3,4-dihydro-1,8-naphthyridine-1(2*H*)-carboxamide (**6k**).

Step 1: *N*-(5-cyano-4-(4-hydroxy-4-methylpiperidin-1-yl)pyridin-2-yl)-7-(dimethoxymethyl)-3,4-dihydro-1,8-naphthyridine-1(2*H*)-carboxamide.

N-(4-chloro-5-cyanopyridin-2-yl)-7-(dimethoxymethyl)-3,4-dihydro-1,8-naphthyridine-1(2*H*)-carboxamide (50 mg, 0.129 mmol) and 4-methylpiperidin-4-ol (21.5 mg, 0.142 mmol) were dissolved in DMF (1 ml) under argon. The mixture was stirred at 100 °C for 16 h. An excess of 4-methylpiperidin-4-ol was added to the mixture and stirred for 45 min at 100 °C. The reaction mixture was diluted in EtOAc and washed 2x with sat. aq. NH₄Cl and brine. The organic layer was dried over Na₂SO₄, filtered and concentrated under vacuum. The crude material was purified by normal phase chromatography (4 g silica gel cartridge, heptanes/EtOAc 100:0 to 0:100) to give 25 mg (39%) of the title compound as an off-white solid.

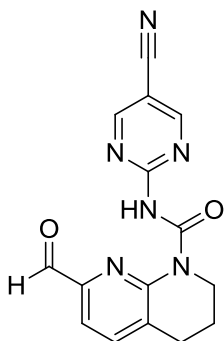
LCMS m/z calculated for C₂₄H₃₀N₆O₄: 466.23, found 467.2 [M+H].

Step 2: *N*-(5-cyano-4-(4-hydroxy-4-methylpiperidin-1-yl)pyridin-2-yl)-7-formyl-3,4-dihydro-1,8-naphthyridine-1(2*H*)-carboxamide (**6k**). *N*-(5-cyano-4-(4-hydroxy-4-methylpiperidin-1-yl)pyridin-

2-yl)-7-formyl-3,4-dihydro-1,8-naphthyridine-1(2*H*)-carboxamide (**6k**). was prepared according to S1 using *N*-(5-cyano-4-(4-hydroxy-4-methylpiperidin-1-yl)pyridin-2-yl)-7-(dimethoxymethyl)-3,4-dihydro-1,8-naphthyridine-1(2*H*)-carboxamide.

¹H NMR (400 MHz, DMSO-*d*₆) δ 13.57 (s, 1H), 9.93 (s, 1H), 8.40 (s, 1H), 7.95 – 7.90 (m, 1H), 7.77 (s, 1H), 7.66 (d, *J* = 7.5 Hz, 1H), 4.49 (s, 1H), 4.02 – 3.94 (m, 2H), 3.67 – 3.58 (m, 2H), 3.43 – 3.35 (m, 2H), 2.94 (t, *J* = 6.3 Hz, 2H), 1.99 – 1.89 (m, 2H), 1.65 – 1.58 (m, 4H), 1.19 (s, 3H).

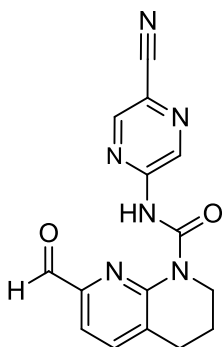
LCMS *m/z* calculated for C₂₂H₂₄N₆O₃: 420.19, found 421.2 [M+H].



N-(5-cyanopyrimidin-2-yl)-7-formyl-3,4-dihydro-1,8-naphthyridine-1(2*H*)-carboxamide (**7a**) was prepared according to S1 using 7-(dimethoxymethyl)-1,2,3,4-tetrahydro-1,8-naphthyridine (**15**) and 2-aminopyrimidine-5-carbonitrile.

¹H NMR (400 MHz, DMSO-*d*₆) δ 14.00 (s, 1H), 9.92 (s, 1H), 9.13 (s, 2H), 7.95 (d, *J* = 7.6 Hz, 1H), 7.68 (d, *J* = 7.6 Hz, 1H), 4.00 – 3.91 (m, 2H), 2.95 (t, 6.3 Hz, 2H), 2.00 – 1.88 (m, 2H).

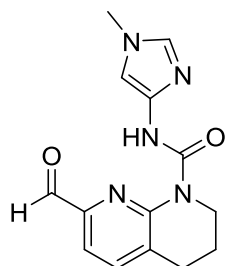
LCMS *m/z* calculated for C₁₅H₁₂N₆O₂: 308.10, found 309.1 [M+H].



N-(5-cyanopyrazin-2-yl)-7-formyl-3,4-dihydro-1,8-naphthyridine-1(2*H*)-carboxamide (7b) was prepared according to S1 using 7-(dimethoxymethyl)-1,2,3,4-tetrahydro-1,8-naphthyridine (15) and 5-aminopyrazine-2-carbonitrile.

¹H NMR (400 MHz, DMSO-*d*₆) δ 14.12 (s, 1H), 9.95 (s, 1H), 9.46 (d, *J* = 1.5 Hz, 1H), 8.99 (d, *J* = 1.5 Hz, 1H), 7.98 (d, *J* = 7.5 Hz, 1H), 7.73 (d, *J* = 7.5 Hz, 1H), 3.99 - 4.05 (m, 2H), 2.96 (t, *J* = 6.3 Hz, 2H), 1.92 - 2.01 (m, 2H).

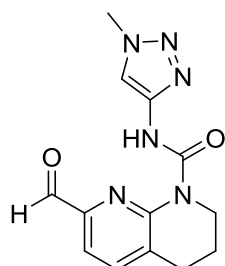
LCMS *m/z* calculated for C₁₅H₁₂N₆O₂: 308.10, found 309.0 [M+H].



7-formyl-*N*-(1-methyl-1*H*-imidazol-4-yl)-3,4-dihydro-1,8-naphthyridine-1(2*H*)-carboxamide (7c) was prepared according to S1 using 7-(dimethoxymethyl)-1,2,3,4-tetrahydro-1,8-naphthyridine (15) and 1-methyl-1*H*-imidazol-4-amine.

¹H NMR (600 MHz, DMSO-*d*₆) δ 12.79 (s, 1H), 9.91 (s, 1H), 7.88 (d, *J* = 7.4 Hz, 1H), 7.62 (d, *J* = 7.4 Hz, 1H), 7.40 (s, 1H), 7.11 (s, 1H), 4.01 - 3.93 (m, 2H), 3.64 (s, 3H), 2.94 (t, *J* = 6.3 Hz, 2H), 1.96-1.89 (m, 2H).

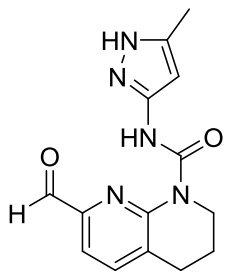
LCMS *m/z* calculated for C₁₄H₁₅N₅O₂: 285.12, found 286.3 [M+H].



7-formyl-*N*-(1-methyl-1*H*-1,2,3-triazol-4-yl)-3,4-dihydro-1,8-naphthyridine-1(2*H*)-carboxamide (7d) was prepared according to S1 using 7-(dimethoxymethyl)-1,2,3,4-tetrahydro-1,8-naphthyridine (15) and 1-methyl-1*H*-1,2,3-triazol-4-amine.

¹H NMR (400 MHz, DMSO-*d*₆) δ 13.25 (s, 1H), 9.94 (s, 1H), 8.05 (s, 1H), 7.91 (d, *J* = 7.5 Hz, 1H), 7.67 (d, *J* = 7.4 Hz, 1H), 4.03 (s, 3H), 4.01 - 3.95 (m, 2H), 2.94 (t, *J* = 6.3 Hz, 2H), 1.93 (p, *J* = 6.2 Hz, 2H).

LCMS m/z calculated for C₁₃H₁₄N₆O₂: 286.12, found 287.2 [M+H].



7-formyl-N-(5-methyl-1H-pyrazol-3-yl)-3,4-dihydro-1,8-naphthyridine-1(2H)-carboxamide (7e).

Step 1: tert-butyl 5-(7-(dimethoxymethyl)-1,2,3,4-tetrahydro-1,8-naphthyridine-1-carboxamido)-3-methyl-1H-pyrazole-1-carboxylate.

tert-butyl 5-(7-(dimethoxymethyl)-1,2,3,4-tetrahydro-1,8-naphthyridine-1-carboxamido)-3-methyl-1H-pyrazole-1-carboxylate was prepared according to S1 using 7-(dimethoxymethyl)-1,2,3,4-tetrahydro-1,8-naphthyridine (**15**) and tert-butyl 5-amino-3-methyl-1H-pyrazole-1-carboxylate.

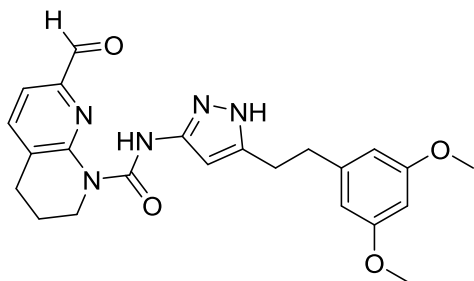
LCMS m/z calculated for C₂₁H₂₉N₅O₅: 431.22, found 432.2 [M+H].

Step 2: 7-formyl-N-(5-methyl-1H-pyrazol-3-yl)-3,4-dihydro-1,8-naphthyridine-1(2H)-carboxamide (**7e**).

Conc. HCl (37% in water, 0.678 ml, 8.25 mmol) was added to a well stirred yellow suspension of tert-butyl 5-(7-(dimethoxymethyl)-1,2,3,4-tetrahydro-1,8-naphthyridine-1-carboxamido)-3-methyl-1H-pyrazole-1-carboxylate (178 mg, 0.413 mmol) in THF (1 ml) and water (1 ml). The resulting solution was stirred at room temperature for 35 min, then quenched with sat. aq. NaHCO₃ and extracted with DCM (3x). The combined organic layers were dried over Na₂SO₄ concentrated. The residue was crystallized from DCM/Et₂O/n-hexane to give 30.7 mg (25%) of the title compound as a slightly pink solid.

¹H NMR (600 MHz, Chloroform-*d*) δ 13.49 (s, 1H), 10.04 (s, 1H), 7.65 (d, *J* = 7.6 Hz, 1H), 7.55 (d, *J* = 7.5 Hz, 1H), 6.24 (s, 1H), 4.10 – 4.07 (m, 2H), 2.93 (t, *J* = 6.4 Hz, 3H), 2.31 (s, 3H), 2.05 – 2.00 (m, 2H).

LCMS m/z calculated for C₁₄H₁₅N₅O₂: 285.12, found 286.2 [M+H].



N-(5-(3,5-dimethoxyphenethyl)-1*H*-pyrazol-3-yl)-7-formyl-3,4-dihydro-1,8-naphthyridine-1(2*H*)-carboxamide (**7f**).

Step 1: tert-butyl 5-amino-3-(3,5-dimethoxyphenethyl)-1*H*-pyrazole-1-carboxylate.

A mixture of 5-[2-(3,5-dimethoxy-phenyl)-ethyl]-1*H*-pyrazol-3-ylamine (1 g, 4.04 mmol), DCM (36 ml) and aq. KOH (4 M, 8.09 ml, 32.4 mmol) was treated dropwise with a solution of di-*tert*-butyl dicarbonate (0.927 g, 4.25 mmol) in DCM (4 ml) and stirred overnight. The reaction mixture was diluted with water and extracted with DCM (2x). The combined organic layers were washed with water and brine, dried over sodium sulfate, filtered and evaporated to yield 1.2 g (77%) of the title compound as a yellow solid.

Step 2: tert-butyl 5-(7-(dimethoxymethyl)-1,2,3,4-tetrahydro-1,8-naphthyridine-1-carboxamido)-3-(3,5-dimethoxyphenethyl)-1*H*-pyrazole-1-carboxylate.

A solution of phosgene (20% solution in toluene, 0.159 ml, 0.302 mmol) in THF (1.5 ml) was treated with NEt₃ (0.100 ml, 0.720 mmol) at room temperature. The resulting white suspension was treated with a solution of 7-(dimethoxymethyl)-1,2,3,4-tetrahydro-1,8-naphthyridine (**15**) (78 mg, 0.374 mmol) in THF (1 ml) via syringe and stirred for 15 min. Then, a solution of tert-butyl 5-amino-3-(3,5-dimethoxyphenethyl)-1*H*-pyrazole-1-carboxylate (100 mg, 0.288 mmol) in THF (0.5 ml) was added and the reaction mixture was stirred overnight. The reaction mixture was treated with sat. aq. NaHCO₃ and extracted with EtOAc (2x). The combined organic layers were washed with brine, dried over sodium sulfate, filtered and evaporated. The crude material was purified by normal phase chromatography (4 g silica gel cartridge, heptanes/EtOAc 100:0 to 0:100) to give 100 mg (60%) of the title compound as a white foam.

LCMS *m/z* calculated for C₃₀H₃₉N₅O₇: 581.28, found 582.4 [M+H].

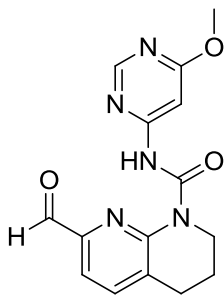
Step 3: *N*-(5-(3,5-dimethoxyphenethyl)-1*H*-pyrazol-3-yl)-7-formyl-3,4-dihydro-1,8-naphthyridine-1(2*H*)-carboxamide (**7f**).

A solution of tert-butyl 5-(7-(dimethoxymethyl)-1,2,3,4-tetrahydro-1,8-naphthyridine-1-carboxamido)-3-(3,5-dimethoxyphenethyl)-1*H*-pyrazole-1-carboxylate (100 mg, 0.172 mmol) in DCM (2.0 ml) was treated with TFA (0.2 ml, 2.60 mmol). After 2 min the reaction was quenched with saturated aq. NaHCO₃ and extracted with DCM (2x). The combined organic layers were

washed with brine, dried over sodium sulfate, filtered and evaporated. The residue was dissolved in MeOH (2.0 ml) and treated with aq. HCl (1 M, 1.0 ml, 1.0 mmol) and stirred for 1 h. The reaction mixture was concentrated, the residue was treated with sat. aq. NaHCO₃ and extracted with DCM (2x). The combined organic layers were washed with brine, dried over sodium sulfate, filtered and evaporated. The residue was dissolved in THF (2.0 ml) and aq. HCl (1 M, 1.0 ml, 1.0 mmol) and stirred for 1h and the concentrated. The residue was treated with sat. aq. NaHCO₃ and extracted with DCM (2x). The combined organic layers were washed with brine, dried over sodium sulfate, filtered and evaporated. The crude material was purified by normal phase chromatography (4 g silica gel cartridge, heptanes/EtOAc 100:0 to 0:100) to give 39 mg (52%) of the title compound as a white foam.

¹H NMR (600 MHz, DMSO-*d*₆) δ 12.95 (s, 1H), 12.04 (s, 1H), 9.89 (s, 1H), 7.88 (d, *J* = 7.5 Hz, 1H), 7.62 (d, *J* = 7.5 Hz, 1H), 6.43 – 6.36 (m, 2H), 6.35 – 6.27 (m, 2H), 3.98 – 3.91 (m, 2H), 3.71 (s, 6H), 2.93 (t, *J* = 6.3 Hz, 2H), 2.89 – 2.82 (m, 4H), 1.95 – 1.89 (m, 2H).

LCMS *m/z* calculated for C₂₃H₂₅N₅O₄: 435.19, found 436.3 [M+H].

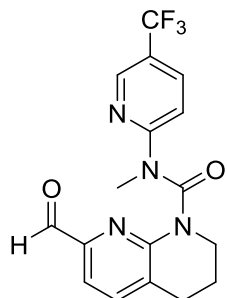


7-formyl-N-(6-methoxypyrimidin-4-yl)-3,4-dihydro-1,8-naphthyridine-1(2H)-carboxamide (7g)

was prepared according to S1 using 7-(dimethoxymethyl)-1,2,3,4-tetrahydro-1,8-naphthyridine (15) and 6-methoxypyrimidin-4-amine.

¹H NMR (400 MHz, DMSO-*d*₆) δ 13.63 (s, 1H), 9.95 (s, 1H), 8.55 (d, 1H), 7.94 (d, *J* = 7.5 Hz, 1H), 7.67 (d, *J* = 7.5 Hz, 1H), 7.41 (d, *J* = 1.0 Hz, 1H), 4.00 – 3.94 (m, 2H), 3.91 (s, 3H), 2.94 (t, *J* = 6.3 Hz, 2H), 2.01 – 1.89 (m, 2H).

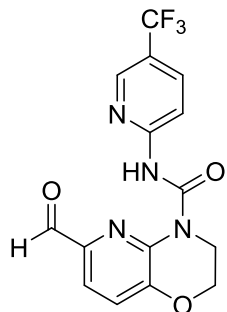
LCMS *m/z* calculated for C₁₅H₁₅N₅O₃: 313.12, found 314.0 [M+H].



7-formyl-N-methyl-N-(5-(trifluoromethyl)pyridin-2-yl)-3,4-dihydro-1,8-naphthyridine-1(2H)-carboxamide (8) was prepared according to S3 using 7-(dimethoxymethyl)-1,2,3,4-tetrahydro-1,8-naphthyridine (**15**) and *N*-methyl-5-(trifluoromethyl)pyridin-2-amine.

^1H NMR (400 MHz, DMSO- d_6) δ 9.57 (s, 1H), 8.47 – 8.43 (m, 1H), 7.83 (dd, J = 8.9, 2.6 Hz, 1H), 7.60 (d, J = 7.5 Hz, 1H), 7.35 (d, J = 8.9 Hz, 1H), 7.29 (d, J = 7.5 Hz, 1H), 3.81 (t, J = 6.0 Hz, 2H), 3.40 (s, 3H), 2.81 (t, J = 6.5 Hz, 2H), 2.08 – 1.94 (m, 2H).

LCMS m/z calculated for $\text{C}_{17}\text{H}_{15}\text{F}_3\text{N}_4\text{O}_2$: 364.11, found 365.0 [M+H].



6-formyl-N-(5-(trifluoromethyl)pyridin-2-yl)-2H-pyrido[3,2-*b*][1,4]oxazine-4(3H)-carboxamide (9).

Step 1: 6-bromo-*N*-(5-(trifluoromethyl)pyridin-2-yl)-2H-pyrido[3,2-*b*][1,4]oxazine-4(3H)-carboxamide. 6-bromo-*N*-(5-(trifluoromethyl)pyridin-2-yl)-2H-pyrido[3,2-*b*][1,4]oxazine-4(3H)-carboxamide was prepared according to S1 using 6-bromo-3,4-dihydro-2H-pyrido[3,2-*b*][1,4]oxazine and 5-(trifluoromethyl)pyridin-2-amine.

LCMS m/z calculated for $\text{C}_{17}\text{H}_{15}\text{F}_3\text{N}_4\text{O}_2$: 364.11, found 365.0 [M+H].

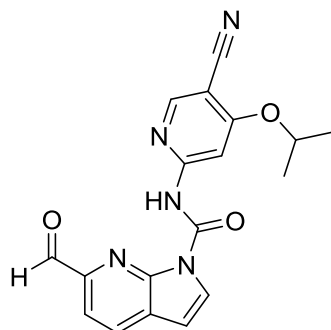
Step 2: 6-formyl-*N*-(5-(trifluoromethyl)pyridin-2-yl)-2H-pyrido[3,2-*b*][1,4]oxazine-4(3H)-carboxamide (**9**).

A suspension of 6-bromo-*N*-(5-(trifluoromethyl)pyridin-2-yl)-2H-pyrido[3,2-*b*][1,4]oxazine-4(3H)-carboxamide (50 mg, 0.124 mmol) in THF (1.5 ml) at -78 °C was treated dropwise with *n*-BuLi (1.38 M in hexanes, 0.225 ml, 0.310 mmol) and the mixture was stirred for 1 h at -78 °C. Then, DMF (0.048 ml, 0.620 mmol) was added and the reaction mixture was stirred for 1 h at -78 °C and then slowly warmed to room temperature. The reaction mixture was quenched with sat. aq.

NH₄Cl and extracted in EtOAc. The org. layer was washed with water, dried over Na₂SO₄, filtered and concentrated. The crude material was purified by normal phase chromatography (4 g silica gel cartridge, heptanes/EtOAc 100:0 to 40:60) to give 11 mg (25%) of the title compound as a white solid.

¹H NMR (400 MHz, DMSO-*d*₆) δ 13.32 (s, 1H) 9.91 (s, 1H) 8.74 - 8.77 (m, 1H) 8.20 - 8.30 (m, 2H) 7.76 (d, *J* = 8.2 Hz, 1H) 7.63 (d, *J* = 8.2 Hz, 1H) 4.42 - 4.47 (m, 2H) 4.13 - 4.19 (m, 2H).

LCMS *m/z* calculated for C₁₅H₁₁F₃N₄O₃: 352.08, found 352.9 [M+H].

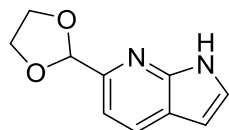


N-(5-cyano-4-isopropoxy-pyridin-2-yl)-6-formyl-1*H*-pyrrolo[2,3-*b*]pyridine-1-carboxamide (10a)

was prepared according to S2 using 6-(1,3-dioxolan-2-yl)-1*H*-pyrrolo[2,3-*b*]pyridine and phenyl (5-cyano-4-isopropoxy-pyridin-2-yl)carbamate.

¹H NMR (600 MHz, DMSO-*d*₆) δ 12.33 (s, 1H), 10.06 (s, 1H), 8.69 (s, 1H), 8.43 (d, *J* = 8.0 Hz, 1H), 8.35 (d, *J* = 4.0 Hz, 1H), 8.00 (d, *J* = 8.0 Hz, 1H), 7.96 (s, 1H), 7.02 (d, *J* = 4.0 Hz, 1H), 4.94 – 4.86 (m, 1H), 1.42 (d, *J* = 6.0 Hz, 6H).

LCMS *m/z* calculated for C₁₈H₁₅N₅O₃: 349.12, found 350.2 [M+H].



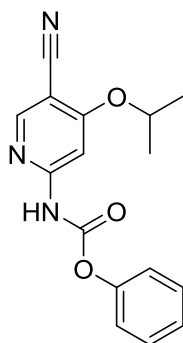
6-(1,3-dioxolan-2-yl)-1*H*-pyrrolo[2,3-*b*]pyridine.

A mixture of 1*H*-pyrrolo[2,3-*b*]pyridine-6-carbaldehyde (840 mg, 5.60 mmol), ethylene glycol (3.13 ml, 56.0 mmol) and propylphosphonic anhydride (50% in EtOAc, 3.34 ml, 5.60 mmol) in EtOAc (15 ml) was stirred at 80 °C. After 18 h, the reaction mixture was cooled to room temperature, diluted with sat. aq. NaHCO₃ and extracted with EtOAc (3x). The combined organic layers were washed with brine, dried over Na₂SO₄ and evaporated. The crude material was applied to a 120 g RediSep® silica column and purified by normal phase chromatography,

eluting with EtOAc. Product-containing fractions were combined and evaporated. The residue was triturated with Et₂O to give 437 mg (37%) the title compound as a white solid.

¹H NMR (600 MHz, DMSO-*d*₆) δ 11.72 (s, 1H), 7.98 (d, *J* = 8.0 Hz, 1H), 7.52 (t, *J* = 3.0 Hz, 1H), 7.21 (d, *J* = 8.0 Hz, 1H), 6.48 – 6.43 (m, 1H), 5.74 (s, 1H), 4.16 – 4.08 (m, 2H), 4.01 – 3.95 (m, 2H).

LCMS *m/z* calculated for C₁₀H₁₀N₂O₂: 190.01, found 191.1 [M+H].

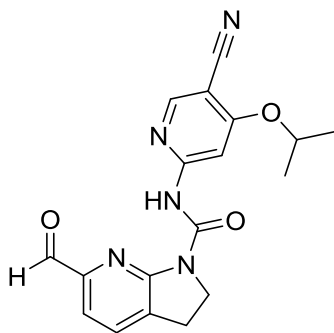


Phenyl (5-cyano-4-isopropoxy)pyridin-2-yl)carbamate.

Phenyl chloroformate (3.89 ml, 31.0 mmol) was added drop wise to a mixture of 6-amino-4-isopropoxynicotinonitrile (2.5 g, 14.11 mmol) and pyridine (2.51 ml, 31.0 mmol) in THF (100 ml) at room temperature. The reaction mixture was stirred for 12 h at room temperature, additional pyridine (2.51 ml, 31.0 mmol) added, before stirring for an additional 12 h and then partitioned between EtOAc and saturated aqueous NaHCO₃ solution. The organic layer was washed with saturated brine, dried over MgSO₄ and evaporated. The residue was triturated with Et₂O and 2.67 g (64%) of the product obtained by filtration as a beige solid.

¹H NMR (400 MHz, DMSO-*d*₆) δ 11.27 (s, 1H), 8.58 (s, 1H), 7.64 (s, 1H), 7.51 – 7.40 (m, 2H), 7.35 – 7.22 (m, 3H), 4.83 – 4.73 (m, 1H), 1.34 (d, *J* = 6.0 Hz, 6H).

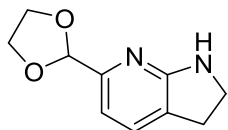
LCMS *m/z* calculated for C₁₆H₁₅N₃O₃: 297.11, found 298.2 [M+H].



N-(5-cyano-4-isopropoxy)pyridin-2-yl)-6-formyl-2,3-dihydro-1*H*-pyrrolo[2,3-*b*]pyridine-1-carboxamide (10b) was prepared according to S2 using crude 6-(1,3-dioxolan-2-yl)-2,3-dihydro-1*H*-pyrrolo[2,3-*b*]pyridine and phenyl (5-cyano-4-isopropoxy)pyridin-2-yl)carbamate.

¹H NMR (400 MHz, DMSO-*d*₆) δ 12.06 (s, 1H), 9.90 (s, 1H), 8.60 (s, 1H), 7.96 (s, 1H), 7.93 (d, *J* = 7.4 Hz, 1H), 7.66 (d, *J* = 7.4 Hz, 1H), 4.84 (m, 1H), 4.14 (m, 2H), 3.23 (m, 2H), 1.40 (d, *J* = 6.1 Hz, 6H).

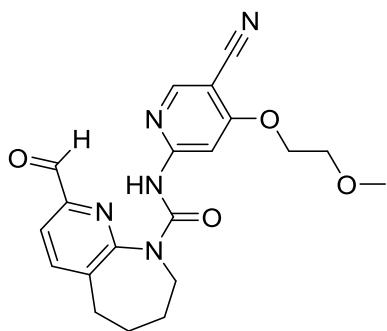
LCMS *m/z* calculated for C₁₈H₁₇N₅O₃: 351.13, found 352.2 [M+H].



6-(1,3-dioxolan-2-yl)-2,3-dihydro-1*H*-pyrrolo[2,3-*b*]pyridine.

A mixture of 6-(1,3-dioxolan-2-yl)-1*H*-pyrrolo[2,3-*b*]pyridine (0.283 g, 1.443 mmol), and Raney nickel (0.140 g) in EtOH (30 ml) was stirred under a hydrogen atmosphere (5 bar) at 95 °C in an autoclave reactor. Additional Raney nickel (0.140 g) was added after 22 h. After 27 h, the reaction mixture was cooled to room temperature, poured onto a glass fiber filter, washed through with additional EtOH and concentrated to give the crude title compound as a brown oil. This material was used without purification in the next step.

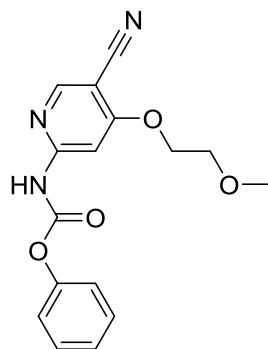
LCMS *m/z* calculated for C₁₀H₁₂N₂O₂: 192.09, found 193.1 [M+H].



N-(5-cyano-4-(2-methoxyethoxy)pyridin-2-yl)-2-formyl-5,6,7,8-tetrahydro-9*H*-pyrido[2,3-*b*]azepine-9-carboxamide (11b) was prepared according to S2 using 2-(dimethoxymethyl)-6,7,8,9-tetrahydro-5*H*-pyrido[2,3-*b*]azepine and phenyl (5-cyano-4-(2-methoxyethoxy)pyridin-2-yl)carbamate.

¹H NMR (400 MHz, DMSO-*d*₆) δ 9.97 (br s, 1H), 9.88 (s, 1H), 8.48 (s, 1H), 8.05 (d, *J* = 7.6 Hz, 1H), 7.86 (s, 1H), 7.85 (d, *J* = 7.6 Hz, 1H), 4.34 (m, 2H), 3.84-3.64 (br m, 2H), 3.75 (m, 2H), 3.35 (s, 3H), 2.91 (m, 2H), 1.82 (m, 2H), 1.72 (m, 2H).

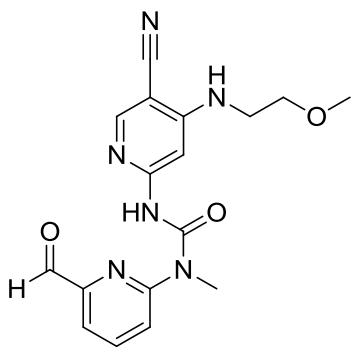
LCMS *m/z* calculated for C₂₀H₂₁N₅O₄: 395.16, found 396.1 [M+H].



Phenyl (5-cyano-4-(2-methoxyethoxy)pyridin-2-yl)carbamate.

Phenyl chloroformate (4.93 ml, 39.3 mmol) was added drop wise to a mixture of 6-amino-4-(2-methoxyethoxy)nicotinonitrile (3.45 g, 17.86 mmol) and pyridine (6.35 ml, 79 mmol) in THF (100 ml) at room temperature. The reaction mixture was stirred for 5 h at room temperature and then partitioned between EtOAc and saturated aqueous NaHCO₃ solution, the organic layer washed with saturated brine, dried over MgSO₄ and evaporated. The residue was triturated with EtOAc and 4.61 g (72%) of the product obtained by filtration as a white solid.

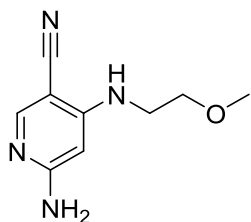
¹H NMR (400 MHz, Chloroform-*d*) δ 9.78 (s, 1H), 8.45 (s, 1H), 7.82 (s, 1H), 7.49 – 7.40 (m, 2H), 7.34 – 7.28 (m, 1H), 7.23 – 7.17 (m, 2H), 4.35 – 4.26 (m, 2H), 3.82 – 3.76 (m, 2H), 3.44 (s, 3H).
LCMS m/z calculated for C₁₆H₁₅N₃O₄: 313.11, found 314.3 [M+H].



3-(5-cyano-4-((2-methoxyethyl)amino)pyridin-2-yl)-1-(6-formylpyridin-2-yl)-1-methylurea (12a) was prepared according to S1 using 6-(1,3-dioxolan-2-yl)-*N*-methylpyridin-2-amine and 6-amino-4-((2-methoxyethyl)amino)nicotinonitrile.

¹H-NMR (400 MHz, DMSO-*d*₆) δ 12.48 (s, 1H), 9.94 (d, *J* = 0.6 Hz, 1H), 8.25 (s, 1H), 8.17 - 8.11 (m, 1H), 7.72 (dd, *J* = 7.5, 0.6 Hz, 1H), 7.68 (m, 1H), 7.47 (s, 1H), 6.97 (t, *J* = 5.6 Hz, 1H), 3.55 - 3.49 (m, 2H), 3.46 (s, 3H), 3.41 – 3.35 (m, 2H), 3.29 (s, 3H).

LCMS m/z calculated for C₁₇H₁₈N₆O₃: 354.14, found 355.1 [M+H].

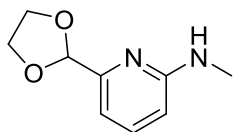


6-amino-4-((2-methoxyethyl)amino)nicotinonitrile.

A solution of 6-amino-4-fluoronicotinonitrile (1.10 g, 8.02 mmol) in DMA (20 ml) was treated with 2-methoxyethylamine (2.07 ml, 24.1 mmol) and DIPEA (4.20 mL, 24.1 mmol), heated to 50 °C and stirred for 15 h. The reaction mixture was cooled to room temperature and concentrated. The crude material was purified by normal phase chromatography (24 g silica gel cartridge, heptanes/EtOAc 100:0 to 0:100). The product containing fractions were concentrated and dried under vacuum to give 1.42 g (90%) of the title compound as an off-white solid.

¹H NMR (400 MHz, DMSO-*d*₆) δ 7.92 (s, 1H), 6.39 (s, 2H), 6.15 (t, *J* = 5.7 Hz, 1H), 5.61 (s, 1H), 3.46 (t, *J* = 5.9 Hz, 2H), 3.27 (s, 3H), 3.24 (q, *J* = 5.9 Hz, 2H).

LCMS *m/z* calculated for C₉H₁₂N₄O: 192.1, found 193.1 [M+H].

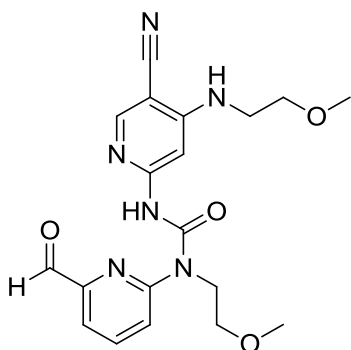


6-(1,3-dioxolan-2-yl)-*N*-methylpyridin-2-amine.

A vial was charged with 2-bromo-6-(1,3-dioxolan-2-yl)pyridine (200 mg, 0.869 mmol), methylamine (2 M in THF, 0.87 ml, 1.7 mmol), chloro[2-(dicyclohexylphosphino)-3,6-dimethoxy-2',4',6'-triisopropyl-1,1'-biphenyl][2-(2-aminoethyl)phenyl]palladium(II) (34.7 mg, 0.043 mmol) and K₂CO₃ (1133 mg, 3.48 mmol), flushed with argon and then charged with *t*-BuOH (4 ml), capped, heated to 110 °C and the mixture stirred for 2 h. The reaction mixture was cooled to room temperature, diluted with water and extracted with EtOAc (2x). The combined organic layers were washed with brine, dried over Na₂SO₄, filtered and concentrated under reduced pressure. The crude material was purified by normal phase chromatography (12 g silica gel cartridge, heptanes/EtOAc 100:0 to 45:55) to give 47.4 mg (29%) of the title compound as a light brown oil.

¹H NMR (400 MHz, DMSO-*d*₆) δ 7.39 (dd, *J* = 8.3, 7.2 Hz, 1H), 6.59 (dd, *J* = 7.2, 0.8 Hz, 1H), 6.54 – 6.46 (m, 1H), 6.40 (dd, *J* = 8.3, 0.8 Hz, 1H), 5.50 (s, 1H), 4.10 – 4.00 (m, 2H), 3.97 – 3.87 (m, 2H), 2.74 (d, *J* = 4.8 Hz, 3H).

LCMS *m/z* calculated for C₉H₁₂N₂O₄: 180.09, found 181.1 [M+H].

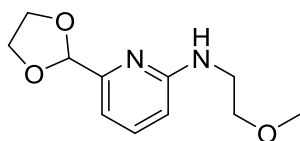


3-(5-cyano-4-((2-methoxyethyl)amino)pyridin-2-yl)-1-(6-formylpyridin-2-yl)-1-(2-

methoxyethyl)urea (12b) was prepared according to S1 using 6-(1,3-dioxolan-2-yl)-*N*-(2-methoxyethyl)pyridin-2-amine and 6-amino-4-((2-methoxyethyl)amino)nicotinonitrile.

^1H NMR (400 MHz, DMSO- d_6) δ 11.44 (s, 1H), 9.92 (s, 1H), 8.24 (s, 1H), 8.08 (t, J = 7.8 Hz, 1H), 7.80 (d, J = 8.5 Hz, 1H), 7.71 (d, J = 7.4 Hz, 1H), 7.39 (s, 1H), 6.97 (t, J = 5.7 Hz, 1H), 4.26 (t, J = 5.4 Hz, 2H), 3.63 (t, J = 5.4 Hz, 2H), 3.55 - 3.49 (m, 2H), 3.40 - 3.36 (m, 2 H), 3.29 - 3.26 (m, 6 H).

LCMS m/z calculated for $\text{C}_{19}\text{H}_{22}\text{N}_6\text{O}_4$: 398.17, found 399.1 [M+H].

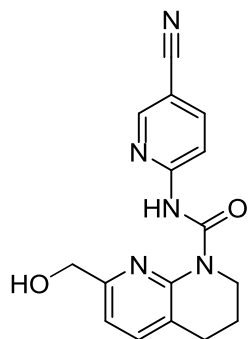


6-(1,3-dioxolan-2-yl)-*N*-(2-methoxyethyl)pyridin-2-amine.

A mixture of 2-bromo-6-(1,3-dioxolan-2-yl)pyridine (210 mg, 0.913 mmol) and 2-methoxyethanamine (1 ml, 11.6 mmol) was heated at 90 °C for 16 h. The reaction mixture was cooled to room temperature and partitioned between water and EtOAc. The aq. layer was extracted with EtOAc (2x). The combined organic layers were dried over Na_2SO_4 , filtered and concentrated under vacuum. The crude material was purified by normal phase chromatography (12 g silica gel cartridge, heptanes/EtOAc 100:0 to 40:60) to give 36 mg (17%) of the title compound as a yellow oil.

^1H NMR (400 MHz, DMSO- d_6) δ 7.37 (dd, J = 8.3, 7.2 Hz, 1H), 6.64 – 6.54 (m, 2H), 6.47 (dd, J = 8.3, 0.8 Hz, 1H), 5.50 (s, 1H), 4.10 – 4.00 (m, 2H), 3.98 – 3.87 (m, 2H), 3.47 – 3.42 (m, 2H), 3.42 – 3.36 (m, 2H), 3.26 (s, 3H).

LCMS m/z calculated for $\text{C}_{11}\text{H}_{16}\text{N}_2\text{O}_3$: 224.12, found 225.2 [M+H].

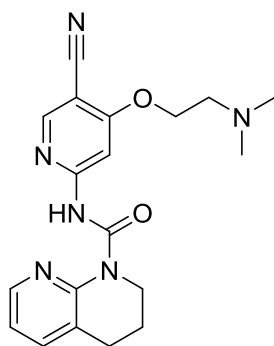


N-(5-cyanopyridin-2-yl)-7-(hydroxymethyl)-3,4-dihydro-1,8-naphthyridine-1(2*H*)-carboxamide (13).

A solution of *N*-(5-cyanopyridin-2-yl)-7-formyl-3,4-dihydro-1,8-naphthyridine-1(2*H*)-carboxamide (**6b**) (22.4 mg, 0.073 mmol) in MeOH (0.5 ml) and DCM (0.5 ml) at room temperature was treated with NaBH₄ (2.2 mg, 0.058 mmol) and stirred for 20 min. The reaction mixture was quenched with sat. aq. NH₄Cl and extracted with DCM (3x). The combined organic layers were dried over Na₂SO₄, filtered and concentrated under reduced pressure. The residue was purified by normal phase chromatography (4 g silica gel cartridge, heptanes/EtOAc 90:10 to 0:100) to give 21 mg (93%) of the title compound as a colorless powder.

¹H NMR (400 MHz, DMSO-*d*₆) δ 14.18 (s, 1H), 8.87- 8.70 (m, 1H), 8.26 - 8.19 (m, 2H), 7.71 (d, *J* = 7.7 Hz, 1H), 7.19 (d, *J* = 7.7 Hz, 1H), 5.55 (t, *J* = 5.8 Hz, 1H), 4.61 (d, *J* = 5.9 Hz, 2H), 3.98 - 3.92 (m, 2H), 2.83 (t, *J* = 6.2 Hz, 2H), 1.87 - 1.96 (m, 2H).

LCMS *m/z* calculated for C₁₆H₁₅N₅O₂: 309.12, found 310.1 [M+H].



N-(5-cyano-4-(2-(dimethylamino)ethoxy)pyridin-2-yl)-3,4-dihydro-1,8-naphthyridine-1(2*H*)-carboxamide (14) was prepared according to S1 using 1,2,3,4-tetrahydro-1,8-naphthyridine and 6-amino-4-(2-(dimethylamino)ethoxy)nicotinonitrile.

^1H NMR (400 MHz, $\text{DMSO-}d_6$) δ 13.96 (s, 1H), 8.54 (s, 1H), 8.27 (dd, $J = 4.9, 1.9$ Hz, 1H), 7.95 (s, 1H), 7.75 – 7.65 (m, 1H), 7.13 (dd, $J = 7.5, 4.9$ Hz, 1H), 4.29 (t, $J = 5.5$ Hz, 2H), 3.99 – 3.90 (m, 2H), 2.85 (t, $J = 6.3$ Hz, 2H), 2.71 (t, $J = 5.5$ Hz, 2H), 2.25 (s, 6H), 1.97 – 1.88 (m, 2H).

LCMS m/z calculated for $\text{C}_{19}\text{H}_{22}\text{N}_6\text{O}_2$: 366.18, found 367.3 [M+H].

X-Ray structure of compound 6b

Table S6. Crystal data and structure refinement for compound 6b.

Identification code	TKN04a	
Empirical formula	C ₁₆ H ₁₃ N ₅ O ₂	
Formula weight	307.31	
Temperature	100(2) K	
Wavelength	1.54178 Å	
Crystal system	Triclinic	
Space group	P-1	
Unit cell dimensions	a = 7.004(2) Å	α = 83.791(11)°
	b = 9.514(3) Å	β = 80.816(11)°
	c = 10.561(3) Å	γ = 89.389(12)°
Volume	690.6(4) Å ³	
Z	2	
Density (calculated)	1.478 g/cm ³	
Absorption coefficient	0.846 mm ⁻¹	
F(000)	320	
Crystal size	0.40 x 0.07 x 0.07 mm ³	
Theta range for data collection	4.27 to 66.59°	
Index ranges	-7<=h<=8, -11<=k<=11, -12<=l<=12	
Reflections collected	13869	
Independent reflections	2392 [R(int) = 0.0309]	
Completeness to theta = 66.59°	98.2 %	
Absorption correction	Semi-empirical from equivalents	
Max. and min. transmission	0.9432 and 0.7285	
Refinement method	Full-matrix least-squares on F ²	
Data / restraints / parameters	2392 / 0 / 208	
Goodness-of-fit on F ²	1.049	
Final R indices [I>2sigma(I)]	R1 = 0.0340, wR2 = 0.0877	
R indices (all data)	R1 = 0.0371, wR2 = 0.0908	
Largest diff. peak and hole	0.186 and -0.261 e.Å ⁻³	

Table S7. Atomic coordinates ($\times 10^4$) and equivalent isotropic displacement parameters ($\text{\AA}^2 \times 10^3$) for TKN04a. $U(\text{eq})$ is defined as one third of the trace of the orthogonalized U_{ij} tensor.

	x	y	z	U(eq)
O(1)	845(1)	1763(1)	6684(1)	26(1)
C(2)	757(2)	2561(1)	7511(1)	21(1)
C(3)	1364(2)	4062(1)	7271(1)	17(1)
C(4)	1311(2)	4856(1)	8292(1)	19(1)
C(5)	1897(2)	6263(1)	8024(1)	18(1)
C(6)	2505(2)	6839(1)	6769(1)	17(1)
C(7)	3058(2)	8375(1)	6463(1)	19(1)
C(8)	2677(2)	8888(1)	5118(1)	19(1)
C(9)	3766(2)	7961(1)	4170(1)	21(1)
N(10)	3118(1)	6461(1)	4474(1)	17(1)
C(11)	2515(2)	5933(1)	5775(1)	16(1)
N(12)	1959(1)	4588(1)	6036(1)	17(1)
C(13)	3297(2)	5710(1)	3384(1)	17(1)
O(14)	3919(1)	6311(1)	2319(1)	24(1)
N(15)	2728(1)	4323(1)	3588(1)	17(1)
C(16)	2742(2)	3393(1)	2656(1)	16(1)
N(17)	1896(1)	2151(1)	3153(1)	17(1)
C(18)	1825(2)	1162(1)	2363(1)	18(1)
C(19)	2617(2)	1343(1)	1058(1)	18(1)
C(20)	3524(2)	2631(1)	554(1)	19(1)
C(21)	3568(2)	3676(1)	1356(1)	19(1)
C(22)	2502(2)	209(1)	280(1)	21(1)
N(23)	2380(2)	-714(1)	-324(1)	29(1)

Table S8. Bond lengths [Å] and angles [°] for TKN04a.

O(1)-C(2)	1.2114(15)
C(2)-C(3)	1.4787(18)
C(2)-H(2)	0.9500
C(3)-N(12)	1.3473(16)
C(3)-C(4)	1.3768(17)
C(4)-C(5)	1.3910(18)
C(4)-H(4)	0.9500
C(5)-C(6)	1.3806(18)
C(5)-H(5)	0.9500
C(6)-C(11)	1.4270(17)
C(6)-C(7)	1.5031(17)
C(7)-C(8)	1.5147(17)
C(7)-H(7A)	0.9900
C(7)-H(7B)	0.9900
C(8)-C(9)	1.5153(17)
C(8)-H(8A)	0.9900
C(8)-H(8B)	0.9900
C(9)-N(10)	1.4884(15)
C(9)-H(9A)	0.9900
C(9)-H(9B)	0.9900
N(10)-C(13)	1.4068(16)
N(10)-C(11)	1.4105(16)
C(11)-N(12)	1.3288(16)
C(13)-O(14)	1.2219(15)
C(13)-N(15)	1.3676(16)
N(15)-C(16)	1.3910(16)
N(15)-H(15)	0.8800
C(16)-N(17)	1.3431(16)
C(16)-C(21)	1.4011(17)
N(17)-C(18)	1.3295(16)
C(18)-C(19)	1.3943(18)
C(18)-H(18)	0.9500

C(19)-C(20)	1.3989(18)
C(19)-C(22)	1.4354(18)
C(20)-C(21)	1.3775(18)
C(20)-H(20)	0.9500
C(21)-H(21)	0.9500
C(22)-N(23)	1.1514(17)

O(1)-C(2)-C(3)	124.51(11)
O(1)-C(2)-H(2)	117.7
C(3)-C(2)-H(2)	117.7
N(12)-C(3)-C(4)	122.99(11)
N(12)-C(3)-C(2)	117.17(10)
C(4)-C(3)-C(2)	119.83(11)
C(3)-C(4)-C(5)	117.97(11)
C(3)-C(4)-H(4)	121.0
C(5)-C(4)-H(4)	121.0
C(6)-C(5)-C(4)	120.59(11)
C(6)-C(5)-H(5)	119.7
C(4)-C(5)-H(5)	119.7
C(5)-C(6)-C(11)	117.39(11)
C(5)-C(6)-C(7)	121.02(11)
C(11)-C(6)-C(7)	121.54(11)
C(6)-C(7)-C(8)	109.29(10)
C(6)-C(7)-H(7A)	109.8
C(8)-C(7)-H(7A)	109.8
C(6)-C(7)-H(7B)	109.8
C(8)-C(7)-H(7B)	109.8
H(7A)-C(7)-H(7B)	108.3
C(7)-C(8)-C(9)	108.97(10)
C(7)-C(8)-H(8A)	109.9
C(9)-C(8)-H(8A)	109.9
C(7)-C(8)-H(8B)	109.9
C(9)-C(8)-H(8B)	109.9
H(8A)-C(8)-H(8B)	108.3

N(10)-C(9)-C(8)	111.31(10)
N(10)-C(9)-H(9A)	109.4
C(8)-C(9)-H(9A)	109.4
N(10)-C(9)-H(9B)	109.4
C(8)-C(9)-H(9B)	109.4
H(9A)-C(9)-H(9B)	108.0
C(13)-N(10)-C(11)	127.64(10)
C(13)-N(10)-C(9)	113.57(10)
C(11)-N(10)-C(9)	118.69(10)
N(12)-C(11)-N(10)	118.15(10)
N(12)-C(11)-C(6)	121.83(11)
N(10)-C(11)-C(6)	120.02(11)
C(11)-N(12)-C(3)	119.23(10)
O(14)-C(13)-N(15)	123.34(11)
O(14)-C(13)-N(10)	119.72(11)
N(15)-C(13)-N(10)	116.94(10)
C(13)-N(15)-C(16)	126.74(10)
C(13)-N(15)-H(15)	116.6
C(16)-N(15)-H(15)	116.6
N(17)-C(16)-N(15)	111.93(10)
N(17)-C(16)-C(21)	122.84(11)
N(15)-C(16)-C(21)	125.20(11)
C(18)-N(17)-C(16)	118.03(10)
N(17)-C(18)-C(19)	123.24(11)
N(17)-C(18)-H(18)	118.4
C(19)-C(18)-H(18)	118.4
C(18)-C(19)-C(20)	118.33(11)
C(18)-C(19)-C(22)	119.57(11)
C(20)-C(19)-C(22)	122.10(11)
C(21)-C(20)-C(19)	118.97(11)
C(21)-C(20)-H(20)	120.5
C(19)-C(20)-H(20)	120.5
C(20)-C(21)-C(16)	118.56(11)
C(20)-C(21)-H(21)	120.7

C(16)-C(21)-H(21)	120.7
N(23)-C(22)-C(19)	178.49(13)

Symmetry transformations used to generate equivalent atoms:

Table S9. Anisotropic displacement parameters ($\text{\AA}^2 \times 10^3$) for TKN04a. The anisotropic displacement factor exponent takes the form: $-2\pi^2 [h^2 a^2 U^{11} + \dots + 2 h k a^* b^* U^{12}]$

	U ¹¹	U ²²	U ³³	U ²³	U ¹³	U ¹²
O(1)	35(1)	21(1)	24(1)	-3(1)	-3(1)	-6(1)
C(2)	21(1)	22(1)	18(1)	1(1)	-2(1)	-1(1)
C(3)	16(1)	19(1)	17(1)	-1(1)	-2(1)	1(1)
C(4)	18(1)	22(1)	15(1)	0(1)	-2(1)	2(1)
C(5)	19(1)	20(1)	18(1)	-5(1)	-4(1)	3(1)
C(6)	14(1)	19(1)	19(1)	-3(1)	-5(1)	2(1)
C(7)	20(1)	18(1)	22(1)	-4(1)	-5(1)	-1(1)
C(8)	21(1)	14(1)	22(1)	-2(1)	-2(1)	-1(1)
C(9)	25(1)	16(1)	21(1)	-1(1)	2(1)	-4(1)
N(10)	20(1)	14(1)	16(1)	-1(1)	0(1)	-2(1)
C(11)	12(1)	17(1)	17(1)	-1(1)	-2(1)	1(1)
N(12)	17(1)	17(1)	16(1)	-1(1)	-1(1)	0(1)
C(13)	16(1)	18(1)	16(1)	-2(1)	-1(1)	1(1)
O(14)	32(1)	20(1)	17(1)	0(1)	3(1)	-4(1)
N(15)	20(1)	16(1)	13(1)	-1(1)	0(1)	-2(1)
C(16)	14(1)	18(1)	17(1)	-2(1)	-4(1)	2(1)
N(17)	17(1)	17(1)	17(1)	-1(1)	-2(1)	0(1)
C(18)	17(1)	16(1)	20(1)	-1(1)	-3(1)	-1(1)
C(19)	18(1)	20(1)	19(1)	-4(1)	-5(1)	2(1)
C(20)	19(1)	22(1)	15(1)	-1(1)	-1(1)	0(1)
C(21)	19(1)	18(1)	18(1)	0(1)	-1(1)	-1(1)
C(22)	20(1)	22(1)	20(1)	-2(1)	-2(1)	0(1)
N(23)	32(1)	28(1)	27(1)	-9(1)	-3(1)	-1(1)

Table S10. Hydrogen coordinates ($\times 10^4$) and isotropic displacement parameters ($\text{\AA}^2 \times 10^3$) for TKN04a.

	x	y	z	U(eq)
H(2)	264	2196	8374	25
H(4)	886	4454	9153	22
H(5)	1880	6834	8710	22
H(7A)	4444	8499	6512	23
H(7B)	2291	8935	7099	23
H(8A)	3111	9883	4887	23
H(8B)	1273	8843	5088	23
H(9A)	3554	8309	3285	25
H(9B)	5169	8022	4198	25
H(15)	2310	3982	4392	20
H(18)	1203	289	2706	22
H(20)	4101	2782	-327	23
H(21)	4145	4570	1034	22

Table S11. Torsion angles [°] for TKN04a.

O(1)-C(2)-C(3)-N(12)	3.59(18)
O(1)-C(2)-C(3)-C(4)	-176.17(11)
N(12)-C(3)-C(4)-C(5)	0.14(18)
C(2)-C(3)-C(4)-C(5)	179.89(11)
C(3)-C(4)-C(5)-C(6)	0.23(18)
C(4)-C(5)-C(6)-C(11)	-0.37(17)
C(4)-C(5)-C(6)-C(7)	177.24(11)
C(5)-C(6)-C(7)-C(8)	-151.51(11)
C(11)-C(6)-C(7)-C(8)	26.00(15)
C(6)-C(7)-C(8)-C(9)	-56.06(13)
C(7)-C(8)-C(9)-N(10)	60.70(13)
C(8)-C(9)-N(10)-C(13)	150.73(10)
C(8)-C(9)-N(10)-C(11)	-32.61(15)
C(13)-N(10)-C(11)-N(12)	-3.16(18)
C(9)-N(10)-C(11)-N(12)	-179.29(10)
C(13)-N(10)-C(11)-C(6)	177.05(10)
C(9)-N(10)-C(11)-C(6)	0.92(16)
C(5)-C(6)-C(11)-N(12)	0.14(17)
C(7)-C(6)-C(11)-N(12)	-177.45(10)
C(5)-C(6)-C(11)-N(10)	179.92(10)
C(7)-C(6)-C(11)-N(10)	2.33(17)
N(10)-C(11)-N(12)-C(3)	-179.57(10)
C(6)-C(11)-N(12)-C(3)	0.21(17)
C(4)-C(3)-N(12)-C(11)	-0.37(18)
C(2)-C(3)-N(12)-C(11)	179.89(10)
C(11)-N(10)-C(13)-O(14)	-177.03(11)
C(9)-N(10)-C(13)-O(14)	-0.73(16)
C(11)-N(10)-C(13)-N(15)	3.74(17)
C(9)-N(10)-C(13)-N(15)	-179.96(10)
O(14)-C(13)-N(15)-C(16)	-0.54(19)
N(10)-C(13)-N(15)-C(16)	178.66(10)
C(13)-N(15)-C(16)-N(17)	-173.17(10)

C(13)-N(15)-C(16)-C(21)	8.28(19)
N(15)-C(16)-N(17)-C(18)	-179.51(9)
C(21)-C(16)-N(17)-C(18)	-0.92(17)
C(16)-N(17)-C(18)-C(19)	1.34(17)
N(17)-C(18)-C(19)-C(20)	-0.27(18)
N(17)-C(18)-C(19)-C(22)	179.01(11)
C(18)-C(19)-C(20)-C(21)	-1.24(17)
C(22)-C(19)-C(20)-C(21)	179.50(11)
C(19)-C(20)-C(21)-C(16)	1.62(17)
N(17)-C(16)-C(21)-C(20)	-0.55(18)
N(15)-C(16)-C(21)-C(20)	177.85(10)
C(18)-C(19)-C(22)-N(23)	14(5)
C(20)-C(19)-C(22)-N(23)	-167(5)

Symmetry transformations used to generate equivalent atoms:

Table S12. Hydrogen bonds for TKN04a [\AA and $^\circ$].

D-H...A	d(D-H)	d(H...A)	d(D...A)	\angle (DHA)
N(15)-H(15)...N(12)	0.88	1.87	2.5944(15)	138.8

Symmetry transformations used to generate equivalent atoms:

Supporting information abbreviations

DSC	differential scanning calorimetry
PAMPA	parallel artificial membrane assay
ATP	adenosine triphosphate
HEPES	4-(2-hydroxy)-1-piperazineethanesulfonic acid
DTT	1,4-dithiothreitol
BSA	bovine serum albumin
EDTA	ethylenediaminetetraacetic acid
Brij35	polyoxyethylene(23)lauryl ether
ELISA	enzyme-linked immunosorbent assay
EGTA	ethylene glycol-bis(β -aminoethyl ether)- <i>N,N,N,N</i> -tetraacetic acid
TBS-T	tris-buffered saline and Tween 20
Mops	3-(<i>N</i> -morpholino)propanesulfonic acid
DCM	dichloromethane
DMAP	4-dimethylaminopyridine
NMP	<i>N</i> -methylpyrrolidinone
THF	tetrahydrofuran
LiHMDS	lithium hexamethyldisilazide
NMP	<i>N</i> -methylpyrrolidone
TFA	trifluoroacetic acid
KHMDS	potassium hexamethyldisilazide
DMF	dimethylformamide
DME	1,2-dimethoxyethane
DIPEA	<i>N,N</i> -diisopropylethylamine

Supporting information references

- 1 Zhou, L.; Yang, L.; Tilton, S.; Wang, J. Development of a high throughput equilibrium solubility assay using a minaturised shake-flask method in early drug discovery. *J. Pharm. Sci.* **2007**, *96*, 3052-3071.
- 2 Wohnsland, F.; Faller, B. High-throughput permeability pH profile and high-throughput alkane/water log *P* with artificial membranes. *J. Med. Chem.* **2001**, *44*, 923-930.
- 3 Giaginis, C.; Theocharis, S.; Tsantili-Kakoulidou, A. Octanol/water partitioning simulation by RP-HPLC for structurally diverse acidic drugs: comparison of three columns in the presence and absence of n-octanol as the mobile phase additive. *J. Sep. Sci.* **2013**, *36*, 3830-3836.
- 4 Bairoch, A.; Boeckmann, B. The SWISS-PROT protein sequence data bank: current status. *Nucleic Acids Res.* **1994**, *22*, 3578-3580.
- 5 Notredame, C.; Higgins, D., G.; Heringa, J. T-Coffee: A novel method for fast and accurate multiple sequence alignment. *J. Mol. Biol.* **2000**, *302*, 205-217.
- 6 Vriend, G. WHAT IF: A molecular modeling and drug design program. *J. Mol. Graph.* **1990**, *8*, 52-56.
- 7 Mohamadi, F.; Richards, N. G. J.; Guida, W. C.; Liskamp, R.; Lipton, M.; Caufield, C.; Chang, G.; Hendrickson, T.; Still, W. C. MacroModel – An integrated software system for modeling organic and bioorganic molecules using molecular mechanics. *J. Comput. Chem.* **1990**, *11*, 440-467.
- 8 Warmuth, M.; Kim, S.; Gu, X.; Xia, G.; Adrián, F. Ba/F3 cells and their use in kinase drug discovery. *Curr. Opin. Onc.* **2007**, *19*, 55-60.
- 9 Melnick, J. S.; Janes, J.; Kim, S.; Chang, J. Y.; Sipes, D. G.; Gunderson, D.; Jarnes, L.; Matzen, J. T.; Garcia, M. E.; Hood, T. L.; Beigi, R.; Xia, G.; Harig, R. A.; Asatryan, H.; Yan, S. F.; Zhou, Y.; Gu, X-J.; Saadat, A.; Zhou, V.; King, F. J.; Shaw, C. M.; Su, A. I.; Downs, R.; Gray, N. S.; Schultz, P. G.; Warmuth, M.; Caldwell, J. S. An efficient rapid system for profiling the cellular activities of molecular libraries PNAS, **2006**, *103*, 3153-3158.
- 10 Neumann, L.; von Konig, K.; Ullmann, D. HTS reporter displacement assay for fragment screening and fragment evolution towards leads with optimized binding kinetics, binding selectivity, and thermodynamic signature. *Method Enzymol.* **2011**, *493*, 299-320.